Relatividade Numérica

Resolvendo as equações de Einstein
no computador

Rafael F. Aranha[1]

[1]Universidade do Estado do Rio de Janeiro
Departamento de Física Teórica
Grupo de Gravitação e Cosmologia

Inverno Astrofísico
Domingos Martins – ES
Setembro/2022

1
Introdução

Relatividade Numérica e Motivação

O que é Relatividade Numérica?

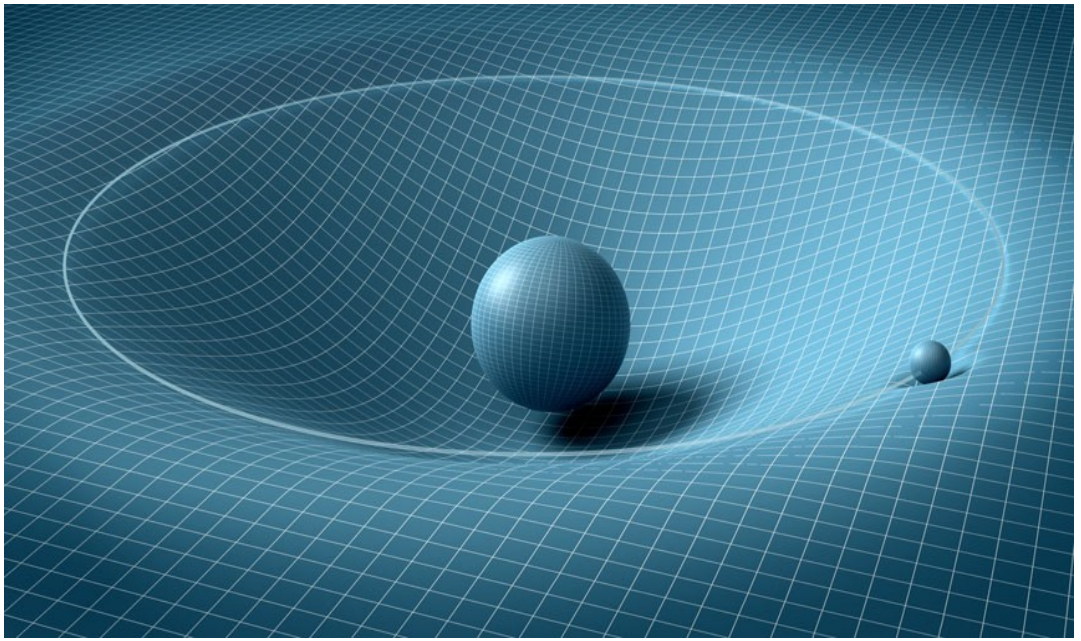

Algoritmo 1: Runge Kutta de 4ª ordem

Entrada: a, b, h, y_0
Saída: x e y como pares de pontos da solução do PVI

início
  $x = a : h : b$
  $n \leftarrow tamanho(x)$
  $y(1) = y_0$
  para $i = 1$ *até* $n - 1$ **faça**
    $k_1 = df(x(i), y(i))$
    $k_2 = df(x(i) + \frac{h}{2}, y(i) + k_1 * \frac{h}{2})$
    $k_3 = df(x(i) + \frac{h}{2}, y(i) + k_2 * \frac{h}{2})$
    $k_4 = df(x(i) + h, y(i) + k_3 * h)$
    $y(i+1) = y(i) + \frac{h}{6} * (k_1 + 2 * k_2 + 2 * k_3 + k_4)$
  fim
fim
retorna (x, y)

Relatividade Geral

+

Métodos Numéricos

O que é Relatividade Numérica?

Computadores aceleram o processo de aquisição de dados.

Algoritmo 1: RUNGE KUTTA DE 4ª ORDEM

Entrada: a, b, h, y_0

Saída: x e y como pares de pontos da solução do PVI

início

- $x = a : h : b$
- $n \leftarrow tamanho(x)$
- $y(1) = y_0$
- **para** $i = 1$ *até* $n - 1$ **faça**
  - $k_1 = df(x(i), y(i))$
  - $k_2 = df(x(i) + \frac{h}{2}, y(i) + k_1 * \frac{h}{2})$
  - $k_3 = df(x(i) + \frac{h}{2}, y(i) + k_2 * \frac{h}{2})$
  - $k_4 = df(x(i) + h, y(i) + k_3 * h)$
  - $y(i+1) = y(i) + \frac{h}{6} * (k_1 + 2 * k_2 + 2 * k_3 + k_4)$
- **fim**

fim

retorna (x, y)

Burden & Faires (2016).

```
def runge_kutta4(f_user, u0, T, n):
    f = lambda u, t:
 np.asarray(f_user(u, t))
    t = np.zeros(n + 1)
    if isinstance(u0, (int, float)):
        u = np.zeros(n + 1)
    else:
        neq = len(u0)
        u = np.zeros((n + 1, neq))
    u[0, :] = u0
    t[0] = 0
    dt = T / n
    dt2 = dt/2

    for i in range(n):
        t[i + 1] = t[i] + dt
        K1 = dt * f(u[i, :], t[i])
        K2 = dt * f(u[i, :] + 0.5 * K1,
             t[i] + dt2)
        K3 = dt * f(u[i, :] + 0.5 * K2,
             t[i] + dt2)
        K4 = dt * f(u[i, :] + K3, t[i]
             + dt)
        u[i + 1, :] = u[i, :] + (1 / 6)
                      * (K1 + 2 * K2 +
                      2 * K3 + K4)
    return u, t
```

Motivação

- Explorar problemas regidos pela interação gravitacional → problemas ilimitados.
- Não-linearidade das equações de Einstein.
- Aplicabilidade em astrofísica relativística e cosmologia.
- Construção de tecnologias computacionais específicas.

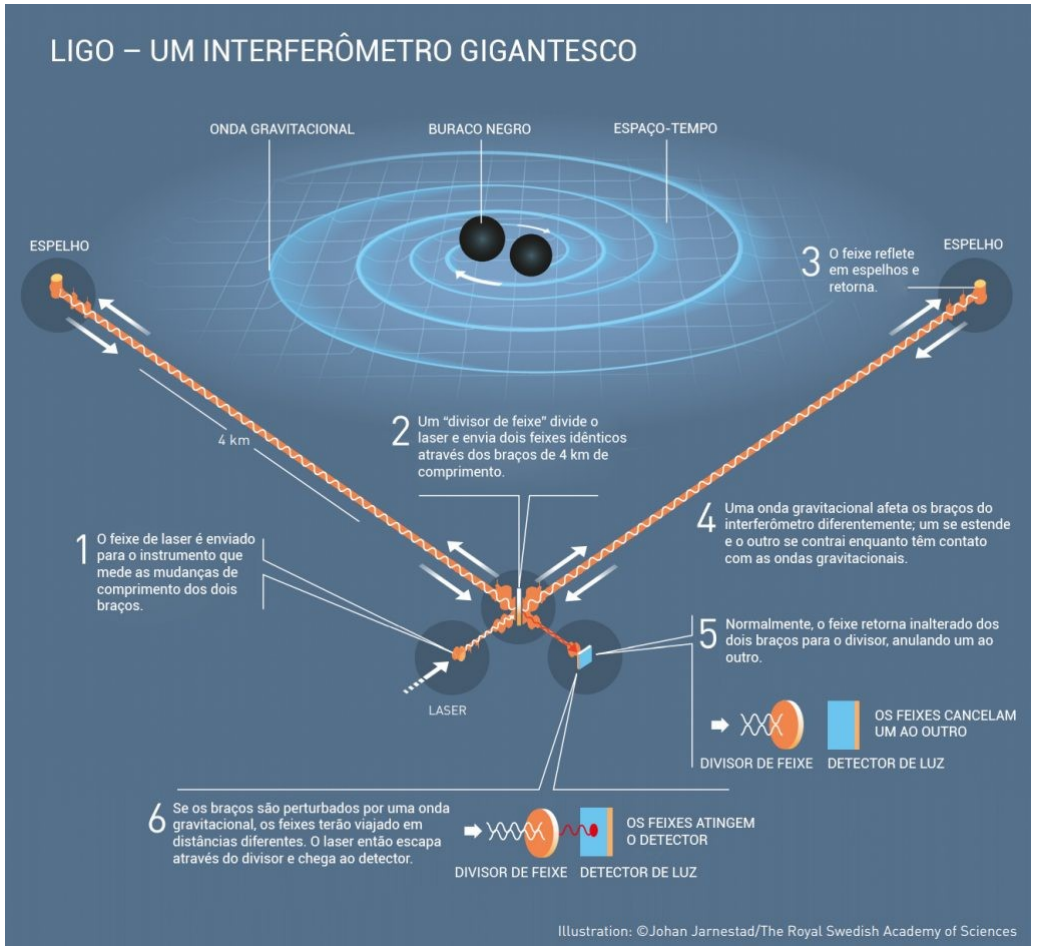

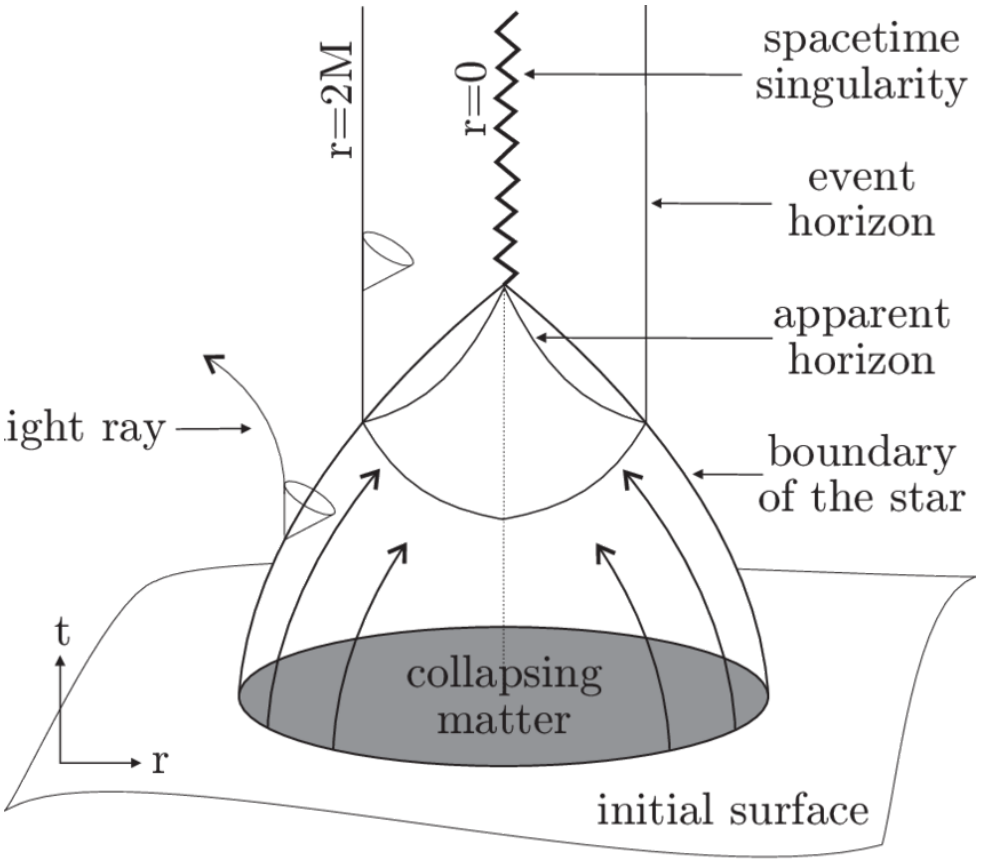

Fonte: Pankaj S. Joshi

Contexto Histórico

Contexto Histórico - 1a Era

- Arnowitt, Deser, Misner (ADM) (1959/62) → Formalismo;

Contexto Histórico - 1a Era

- Arnowitt, Deser, Misner (ADM) (1959/62) → Formalismo;
- Hahn, Lindquist (1964) → Dados Iniciais de Misner;

ANNALS OF PHYSICS: 29, 304–331 (1964)

The Two-Body Problem in Geometrodynamics

SUSAN G. HAHN

International Business Machines Corporation, New York, New York

AND

RICHARD W. LINDQUIST

Contexto Histórico - 1a Era

- Arnowitt, Deser, Misner (ADM) (1959/62) → Formalismo;
- Hahn, Lindquist (1964) → Dados Iniciais de Misner;

ANNALS OF PHYSICS: 29, 304–331 (1964)

The Two-Body Problem in Geometrodynamics

SUSAN G. HAHN

International Business Machines Corporation, New York, New York

AND

RICHARD W. LINDQUIST

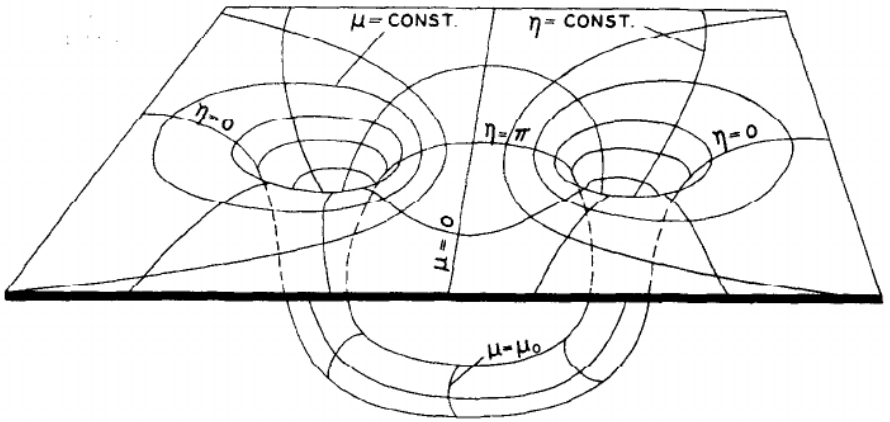

- Dado inicial de Misner (1960) e o computador IBM 7090.

Contexto Histórico - 1a Era

- Smarr (1976) → Colisão entre dois buracos negros

PHYSICAL REVIEW D VOLUME 14, NUMBER 10 15 NOVEMBER 1976

Collision of two black holes: Theoretical framework*

Larry Smarr
Princeton University Observatory, Princeton, New Jersey 08540

Andrej Čadež
Univerza v Ljubljani, Fakulteta za Naravoslovje in Tehnologijo, Odsek za Fiziko, 61000 Ljubljana, Yugoslavia

Bryce DeWitt
Center for Relativity, Department of Physics, University of Texas, Austin, Texas 78712

Kenneth Eppley
Department of Physics and Astronomy University of North Carolina, Chapel Hill, North Carolina 27514
(Received 21 June 1976)

Highly nonspherical time-dependent collisions between black holes may be powerful sources of gravitational radiation. We consider various attempts at estimating the efficiency of the generation of radiation by such collisions. To determine the actual efficiency as well as to understand the details of the dynamical coalescence of black-hole event horizons, we have developed a numerical method for solving the Einstein gravitational field equations in these high-velocity strong-field regions. The head-on collision of two nonrotating vacuum black holes is chosen as an example of our technique. We use the geometrodynamical model of a black hole as an Einstein-Rosen bridge. The initial data to be evolved are the time-symmetric conformally flat data discovered by Misner. A new set of spatial coordinates for these data is derived. Then the general space plus time decomposition of Einstein's equations is presented and specialized to the axisymmetric nonrotating case. Details of the evolution will be given in later papers.

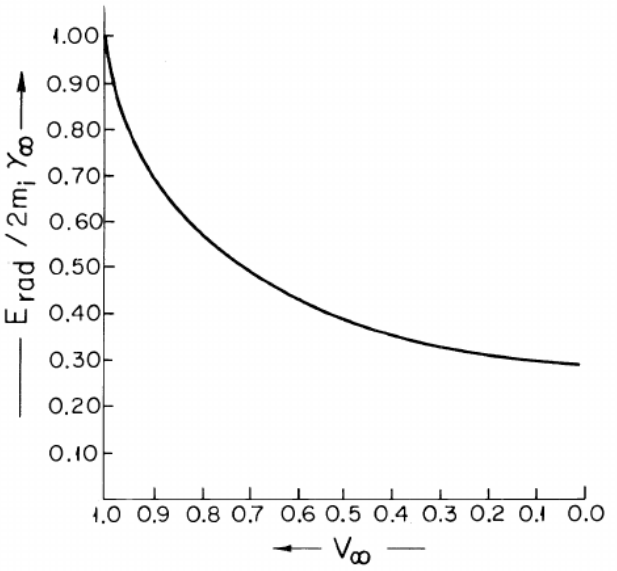

FIG. 1. The upper limit (using the Hawking area increase theorem) on the efficiency of conversion of the energy of two colliding black holes with hyperbolic velocities to gravitational radiation. The initial velocity at infinite separation (v_∞) is plotted horizontally and the efficiency ($E_{rad}/2m_i\gamma_\infty$) is plotted vertically.

Contexto Histórico - 1a Era

- Eppley (1977) → Ondas de Brill e horizontes aparentes

PHYSICAL REVIEW D VOLUME 16, NUMBER 6 15 SEPTEMBER 1977

Evolution of time-symmetric gravitational waves: Initial data and apparent horizons*

Kenneth Eppley
University of Maryland, College Park, Maryland
(Received 4 March 1977)

Initial data were constructed numerically representing pure gravitational radiation with no sources or wormholes, under the conditions of time symmetry, axisymmetry, vacuum, and no rotation. The constraints were solved by making a conformal transformation on a base metric and solving the scale equation for the conformal factor. The initial data contain a black hole if the amplitude of the waves is sufficiently strong. The locations of apparent horizons were found for several such amplitudes. At a critical amplitude the throat pinches off and the geometry becomes singular.

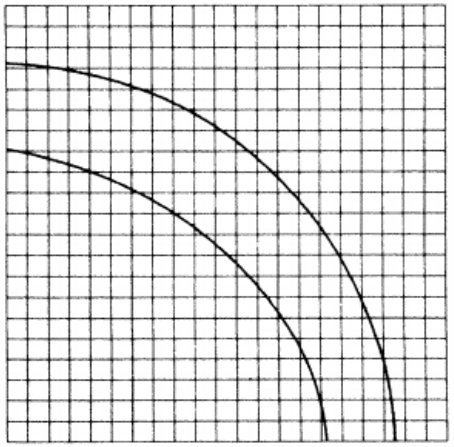

FIG. 3. Location of apparent horizons. The inner curve is for $A=5$, where the horizon first appears. The outer curve is for $A=15$, just before the pinch-off (shown for $\lambda=1$, $n=5$, step size of 0.05).

Contexto Histórico - 1a Era

- Smarr, Wilson, Piran (1978) → Seattle conference

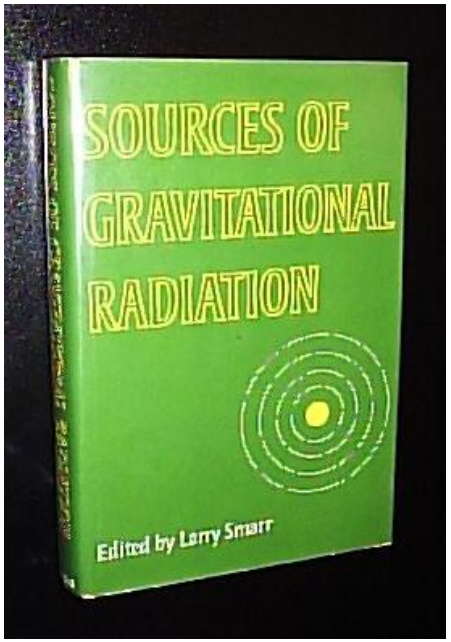

CONTENTS

Contexto Histórico - 1a Era

- Smarr, Wilson, Piran (1978) → Seattle conference

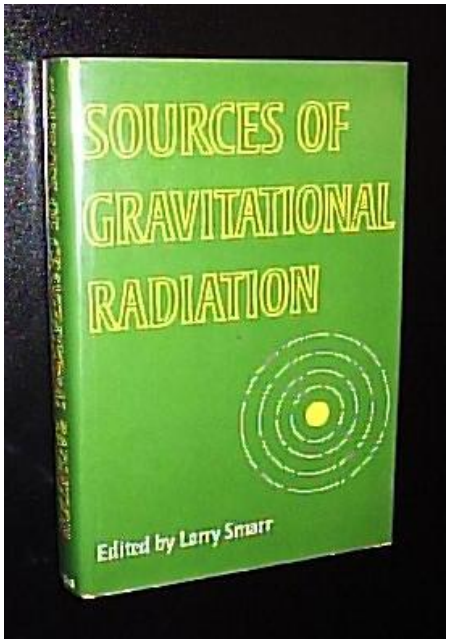

CONTENTS

Contexto Histórico - 1a Era

- Smarr, Wilson, Piran (1978) → Seattle conference

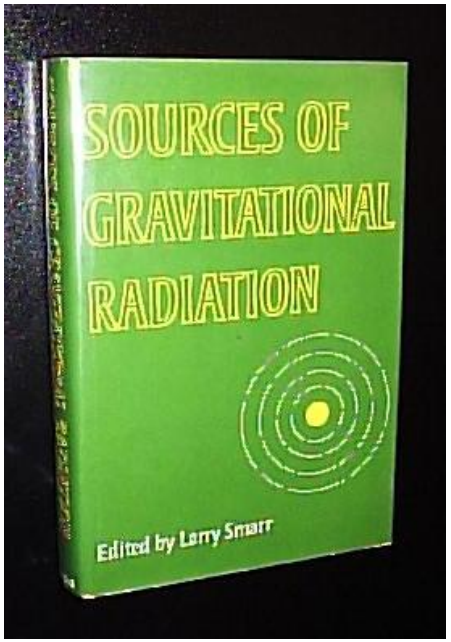

CONTENTS

Contexto Histórico - 1a Era

- Smarr, Wilson, Piran (1978) → Seattle conference

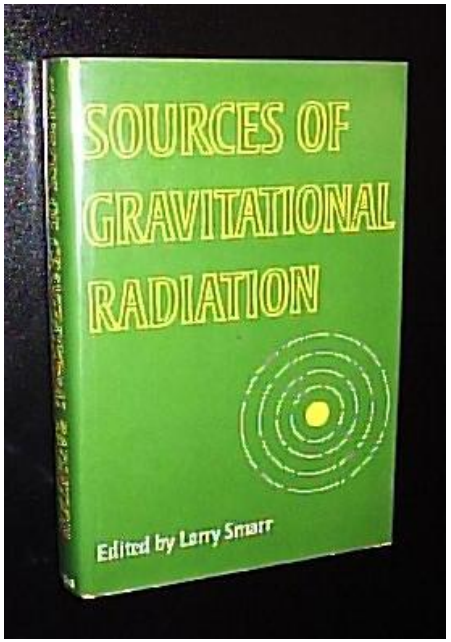

Falta de recursos computacionais

CONTENTS

Contexto Histórico - 2a Era

- BBH Grand Challenge Alliance (1995); Lazarus (1998-2005).

12th 'Kingston meeting': Computational Astrophysics
ASP Conference Series Vol. 123, 1997
David A. Clarke & Michael J. West (eds.)

The Binary Black Hole Grand Challenge Project

M. W. Choptuik

Center for Relativity, Department of Physics, University of Texas at Austin, Austin, TX 78712-1081, U.S.A.

Abstract. The status of the Binary Black Hole Grand Challenge project is reviewed. This effort, which has involved over 40 researchers at 10 institutions, aims to simulate the in-spiral and merger of black hole binaries, and to provide predicted gravitational waveforms from such events. Conceivably, radiation from black-hole mergers could be detected within the next decade by the new generation of large scale gravitational wave detectors currently under construction. This report summarizes advances which have been made on physical, mathematical and computational aspects of the problem, and outlines some of the key hurdles which remain.

BBHGC: Interdisciplinar, HPC.

Lazarus: Unificação de métodos (Pert, PN, NumRel).

PHYSICAL REVIEW D, VOLUME 65, 044001

The Lazarus project: A pragmatic approach to binary black hole evolutions

John Baker
Albert-Einstein-Institut, Max-Planck-Institut für Gravitationsphysik, Am Mühlenberg 1, D-14476 Golm, Germany and Laboratory for High Energy Astrophysics, NASA Goddard Space Flight Center, Greenbelt, Maryland 20771

Manuela Campanelli
Albert-Einstein-Institut, Max-Planck-Institut für Gravitationsphysik, Am Mühlenberg 1, D-14476 Golm, Germany and Department of Physics and Astronomy, The University of Texas at Brownsville, Brownsville, Texas 78520

Carlos O. Lousto
Albert-Einstein-Institut, Max-Planck-Institut für Gravitationsphysik, Am Mühlenberg 1, D-14476 Golm, Germany; Department of Physics and Astronomy, The University of Texas at Brownsville, Brownsville, Texas 78520; and Instituto de Astronomía y Física del Espacio–CONICET, Buenos Aires, Argentina
(Received 19 April 2001; published 7 January 2002)

We present a detailed description of techniques developed to combine 3D numerical simulations and, subsequently, a single black hole close-limit approximation. This method has made it possible to compute the first complete waveforms covering the post-orbital dynamics of a binary–black-hole system with the numerical simulation covering the essential nonlinear interaction before the close limit becomes applicable for the late time dynamics. In order to couple full numerical and perturbative methods we must address several questions. To determine when close-limit perturbation theory is applicable we apply a combination of invariant *a priori* estimates and *a posteriori* consistency checks of the robustness of our results against exchange of linear and nonlinear treatments near the interface. Our method begins with a specialized application of standard numerical techniques adapted to the presently realistic goal of brief, but accurate simulations. Once the numerically modeled binary system reaches a regime that can be treated as perturbations of the Kerr spacetime, we must approximately relate the numerical coordinates to the perturbative background coordinates. We also perform a rotation of a numerically defined tetrad to asymptotically reproduce the tetrad required in the perturbative treatment. We can then produce numerical Cauchy data for the close-limit evolution in the form of the Weyl scalar ψ_4 and its time derivative $\partial_t\psi_4$ with both objects being first order coordinate and tetrad invariant. The Teukolsky equation in Boyer-Lindquist coordinates is adopted to further continue the evolution. To illustrate

Contexto Histórico - 2a Era

- BBH Grand Challenge Alliance (1995); Lazarus (1998-2005).

12th 'Kingston meeting': Computational Astrophysics
ASP Conference Series Vol. 123, 1997
David A. Clarke & Michael J. West (eds.)

The Binary Black Hole Grand Challenge Project

M. W. Choptuik

Center for Relativity, Department of Physics, University of Texas at Austin, Austin, TX 78712-1081, U.S.A.

Abstract. The status of the Binary Black Hole Grand Challenge project is reviewed. This effort, which has involved over 40 researchers at 10 institutions, aims to simulate the in-spiral and merger of black hole binaries, and to provide predicted gravitational waveforms from such events. Conceivably, radiation from black-hole mergers could be detected within the next decade by the new generation of large scale gravitational wave detectors currently under construction. This report summarizes advances which have been made on physical, mathematical and computational aspects of the problem, and outlines some of the key hurdles which remain.

BBHGC: Interdisciplinar, HPC.

Lazarus: Unificação de métodos (Pert, PN, NumRel).

PHYSICAL REVIEW D, VOLUME 65, 044001

The Lazarus project: A pragmatic approach to binary black hole evolutions

John Baker
Albert-Einstein-Institut, Max-Planck-Institut für Gravitationsphysik, Am Mühlenberg 1, D-14476 Golm, Germany and Laboratory for High Energy Astrophysics, NASA Goddard Space Flight Center, Greenbelt, Maryland 20771

Manuela Campanelli
Albert-Einstein-Institut, Max-Planck-Institut für Gravitationsphysik, Am Mühlenberg 1, D-14476 Golm, Germany and Department of Physics and Astronomy, The University of Texas at Brownsville, Brownsville, Texas 78520

Carlos O. Lousto
Albert-Einstein-Institut, Max-Planck-Institut für Gravitationsphysik, Am Mühlenberg 1, D-14476 Golm, Germany; Department of Physics and Astronomy, The University of Texas at Brownsville, Brownsville, Texas 78520; and Instituto de Astronomía y Física del Espacio–CONICET, Buenos Aires, Argentina
(Received 19 April 2001; published 7 January 2002)

We present a detailed description of techniques developed to combine 3D numerical simulations and, subsequently, a single black hole close-limit approximation. This method has made it possible to compute the first complete waveforms covering the post-orbital dynamics of a binary–black-hole system with the numerical simulation covering the essential nonlinear interaction before the close limit becomes applicable for the late time dynamics. In order to couple full numerical and perturbative methods we must address several questions. To determine when close-limit perturbation theory is applicable we apply a combination of invariant *a priori* estimates and *a posteriori* consistency checks of the robustness of our results against exchange of linear and nonlinear treatments near the interface. Our method begins with a specialized application of standard numerical techniques adapted to the presently realistic goal of brief, but accurate simulations. Once the numerically modeled binary system reaches a regime that can be treated as perturbations of the Kerr spacetime, we must approximately relate the numerical coordinates to the perturbative background coordinates. We also perform a rotation of a numerically defined tetrad to asymptotically reproduce the tetrad required in the perturbative treatment. We can then produce numerical Cauchy data for the close-limit evolution in the form of the Weyl scalar ψ_4 and its time derivative $\partial_t\psi_4$ with both objects being first order coordinate and tetrad invariant. The Teukolsky equation in Boyer-Lindquist coordinates is adopted to further continue the evolution. To illustrate

Formalismo matemático não permite evoluções estáveis!

Contexto Histórico - Pretorius e a 3a Era

PRL **95,** 121101 (2005) PHYSICAL REVIEW LETTERS week ending 16 SEPTEMBER 2005

Evolution of Binary Black-Hole Spacetimes

Frans Pretorius[1,2,*]

[1]*Theoretical Astrophysics, California Institute of Technology, Pasadena, California 91125, USA*
[2]*Department of Physics, University of Alberta, Edmonton, AB T6G 2J1 Canada*

(Received 6 July 2005; published 14 September 2005)

We describe early success in the evolution of binary black-hole spacetimes with a numerical code based on a generalization of harmonic coordinates. Indications are that with sufficient resolution this scheme is capable of evolving binary systems for enough time to extract information about the orbit, merger, and gravitational waves emitted during the event. As an example we show results from the evolution of a binary composed of two equal mass, nonspinning black holes, through a single plunge orbit, merger, and ringdown. The resultant black hole is estimated to be a Kerr black hole with angular momentum parameter $a \approx 0.70$. At present, lack of resolution far from the binary prevents an accurate estimate of the energy emitted, though a rough calculation suggests on the order of 5% of the initial rest mass of the system is radiated as gravitational waves during the final orbit and ringdown.

Pretorius

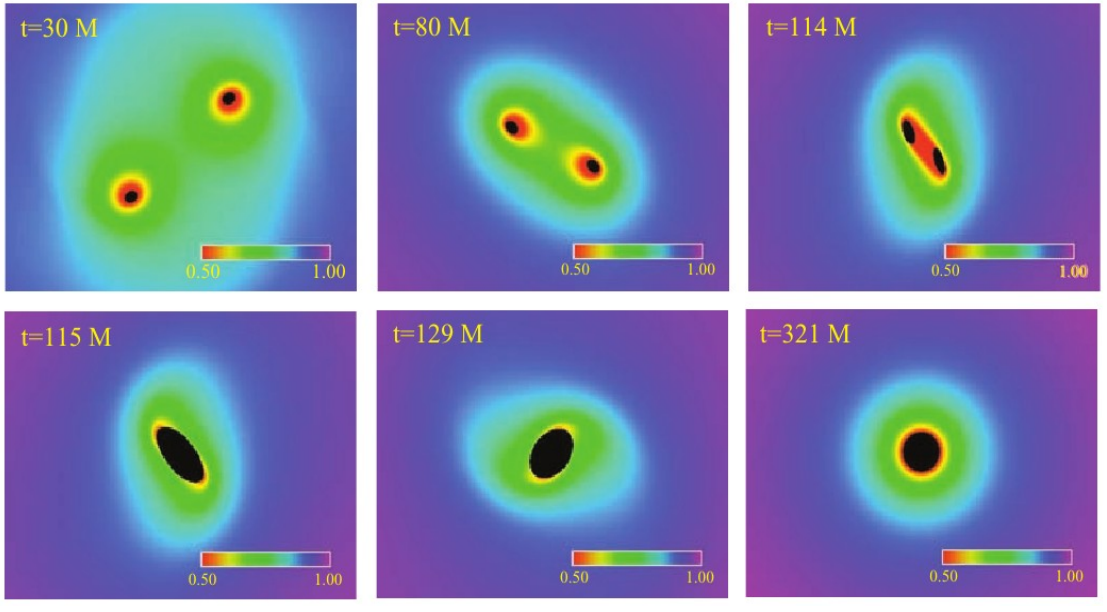

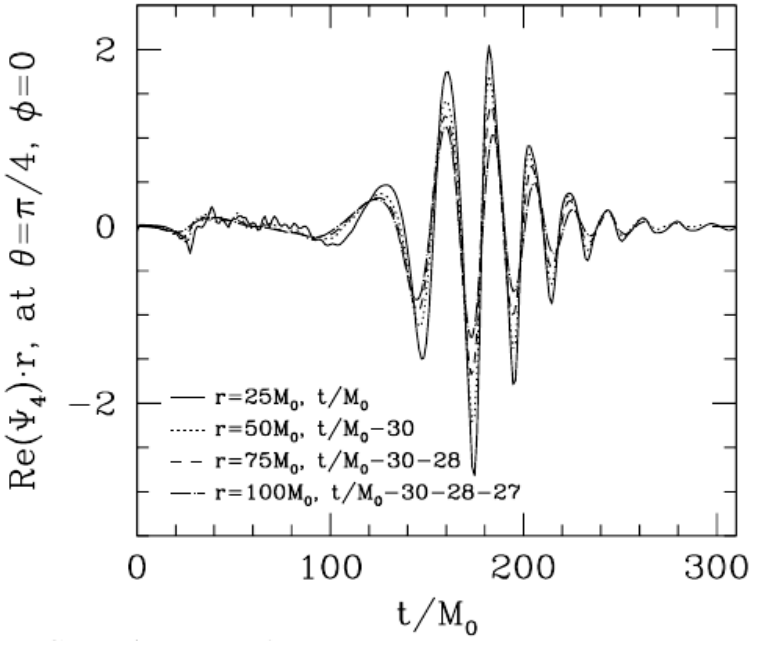

Contexto Histórico - 06' papers

PRL 96, 111101 (2006) PHYSICAL REVIEW LETTERS week ending 24 MARCH 2006

Accurate Evolutions of Orbiting Black-Hole Binaries without Excision

M. Campanelli, C. O. Lousto,[1] P. Marronetti,[2] and Y. Zlochower[1]

[1]*Department of Physics and Astronomy, and Center for Gravitational Wave Astronomy, The University of Texas at Brownsville, Brownsville, Texas 78520, USA*

[2]*Department of Physics, Florida Atlantic University, Boca Raton, Florida 33431, USA*

(Received 9 November 2005; published 22 March 2006)

We present a new algorithm for evolving orbiting black-hole binaries that does not require excision or a corotating shift. Our algorithm is based on a novel technique to handle the singular puncture conformal factor. This system, based on the Baumgarte-Shapiro-Shibata-Nakamura formulation of Einstein's equations, when used with a "precollapsed" initial lapse, is nonsingular at the start of the evolution and remains nonsingular and stable provided that a good choice is made for the gauge. As a test case, we use this technique to fully evolve orbiting black-hole binaries from near the innermost stable circular orbit regime. We show fourth-order convergence of waveforms and compute the radiated gravitational energy and angular momentum from the plunge. These results are in good agreement with those predicted by the Lazarus approach.

DOI: 10.1103/PhysRevLett.96.111101 PACS numbers: 04.25.Dm, 04.25.Nx, 04.30.Db, 04.70.Bw

Campanelli

PRL 96, 111102 (2006) PHYSICAL REVIEW LETTERS week ending 24 MARCH 2006

Gravitational-Wave Extraction from an Inspiraling Configuration of Merging Black Holes

John G. Baker,[1] Joan Centrella,[1] Dae-Il Choi,[1,2] Michael Koppitz,[1] and James van Meter[1]

[1]*Gravitational Astrophysics Laboratory, NASA Goddard Space Flight Center, 8800 Greenbelt Road, Greenbelt, Maryland 20771, USA*

[2]*Universities Space Research Association, 10211 Wincopin Circle, Suite 500, Columbia, Maryland 21044, USA*

(Received 15 November 2005; published 22 March 2006)

We present new ideas for evolving black holes through a computational grid without excision, which enable accurate and stable evolutions of binary black hole systems with the accurate determination of gravitational waveforms directly from the wave zone region. Rather than excising the black hole interiors, our approach follows the "puncture" treatment of black holes, but utilizing a new gauge condition which allows the black holes to move successfully through the computational domain. We apply these techniques to an inspiraling binary, modeling the radiation generated during the final plunge and ringdown. We demonstrate convergence of the waveforms and good conservation of mass-energy, with just over 3% of the system's mass converted to gravitational radiation.

DOI: 10.1103/PhysRevLett.96.111102 PACS numbers: 04.25.Dm, 04.30.Db, 04.70.Bw, 95.30.Sf

Centrella

Contexto Histórico - 2015 General Relativity's Centennial

- Relatividade Numérica como destaque.

IStockphoto.com/Andy_R

General Relativity on a Computer

Only in rare cases can the highly nonlinear equations of general relativity be solved analytically. Many interesting questions in general relativity call for approximations and computational techniques that yield accurate answers when analytic methods are not available. Two seminal successes in answering that call are the Choptuik scaling laws of gravitational collapse and the three papers that revolutionized numerical relativity.

Universality and scaling in gravitational collapse of a massless scalar field
Matthew W. Choptuik
Phys. Rev. Lett. **70**, 9 (1993)

Evolution of Binary Black-Hole Spacetimes
Frans Pretorius
Phys. Rev. Lett. **95**, 121101 (2005)

Accurate Evolutions of Orbiting Black-Hole Binaries without Excision
M. Campanelli, C. O. Lousto, P. Marronetti, and Y. Zlochower
Phys. Rev. Lett. **96**, 111101 (2006)

Gravitational-Wave Extraction from an Inspiraling Configuration of Merging Black Holes
John G. Baker, Joan Centrella, Dae-Il Choi, Michael Koppitz, and James van Meter
Phys. Rev. Lett. **96**, 111102 (2006)

Contexto Histórico - Detecção de OGs - 11/02/16 - 13h:30m (DF)

CBS NEWS NEWS SHOWS VIDEO CBSN MORE

By WILLIAM HARWOOD / CBS NEWS / *February 11, 2016, 11:45 AM*

Einstein was right: Scientists detect gravitational waves in breakthrough

Last Updated Feb 11, 2016 6:59 PM EST

A century after Albert Einstein predicted their existence, gravitational waves have finally been detected, tiny ripples in the fabric of space-time that were generated when two massive black holes, spinning around each other and radiating away gravitational energy, crashed together in a space-warping cataclysm, scientists announced Thursday.

At a packed news briefing at the National Press Club in Washington, researchers unveiled the results of recent observations using the U.S.-led Laser Interferometer

Found! Gravitational Waves, or a Wrinkle in Spacetime

Ripples produced by enormous cosmic events could open a new era in astronomy.

At a packed news briefing at the National Press Club in Washington, researchers unveiled the results of recent observations using the U.S.-led Laser Interferometer

Contexto Histórico - Detecção de OGs - Impacto na Mídia

CBS NEWS NEWS SHOWS VIDEO CBSN MORE

NATIONAL GEOGRAPHIC | LATEST STORIES | TV | PHOTO OF THE DAY |

SECTIONS HOME SEARCH The New York Times

SCIENCE

Scientists Chirp Excitedly for LIGO, Gravitational Waves and Einstein

Trilobites

By MICHAEL ROSTON FEB. 11, 2016

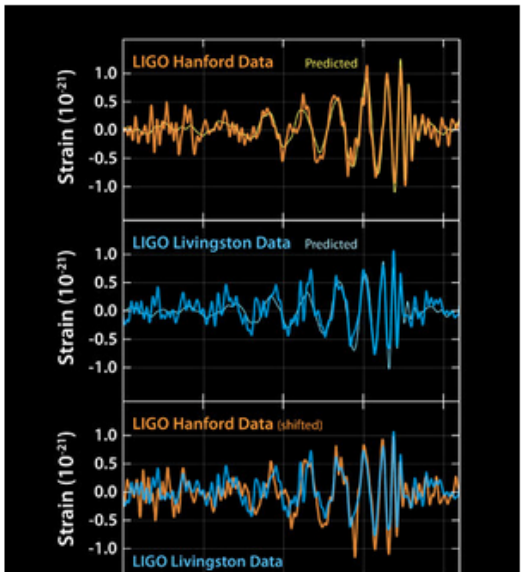

How do you celebrate a major discovery in physics and astronomy that could change the shape of scientific inquiry for the next century? Many scientists active on social media did it by chirping.

Evidence of gravitational waves was announced on Thursday by physicists associated with the Laser Interferometer Gravitational-Wave Observatory project. The experiment's two L-shaped antennas, in Louisiana and Washington state, detected a signal in September that

RELATED COVERAGE

OUT THERE

Gravitational Waves Detected, Confirmin Einstein's Theory FEB. 11, 2016

LIGO Hears Gravitational Waves Einstei Predicted FEB. 11, 2016

Contexto Histórico - Detecção de OGs - Impacto na Mídia

CBS NEWS NEWS SHOWS VIDEO CBSN MORE

NATIONAL GEOGRAPHIC | LATEST STORIES | TV | PHOTO OF THE DAY |

SECTIONS HOME SEARCH The New York Times

Privacy and cookies | Jobs | Dating | Offers | Shop | Puzzles | Investor | Log in | Register | Subscribe

The Telegraph

Search - enhanced by Google

Monday 14 August 2017

Home Video News World Sport Business Money Comment Culture Travel Life Women Fashion Luxury Tech Film

Politics | Investigations | Obits | Education | Science | Earth | Weather | Health | Royal | Celebrity | Defence | Scotland

Science News | Dinosaurs | Space | Night Sky | Evolution | Picture Galleries | Science Video

HOME » NEWS » SCIENCE » SCIENCE NEWS

Moment scientists reveal major gravitational wave finding

Scientists confirm Albert Einstein's 100-year-old prediction of the existence of gravitational waves was right

The Telegraph

Curtir Página 4,3 M curtidas

Related Video

Scientists observe first seconds of universe

18 Mar 2014

What is a gravitational wave?

Confirmin

ves Einstei

Contexto Histórico - Detecção de OGs - Impacto na Mídia

CBS NEWS NEWS SHOWS VIDEO CBSN MORE

NATIONAL GEOGRAPHIC | LATEST STORIES | TV | PHOTO OF THE DAY |

SECTIONS HOME SEARCH The New York Times

Privacy and cookies | Jobs | Dating | Offers | Shop | Puzzles | Investor | Log in | Register | Subscribe

The Telegraph

Search - enhanced by Google

Monday 14 August 2017

BBC Sign in News Sport Weather Shop Earth Travel More Search

NEWS

Home | Video | World | UK | Business | Tech | Science | Magazine | Entertainment & Arts | Health | World News TV | More

Science & Environment

Einstein's gravitational waves 'seen' from black holes

By Pallab Ghosh
Science correspondent, BBC News

11 February 2016 | Science & Environment Share

Contexto Histórico - Detecção de OGs - Impacto na Mídia

Gravitational waves: breakthrough discovery after a century of expectation

Scientists announce discovery of clear gravitational wave signal, ripples in spacetime first predicted by Albert Einstein

Contexto Histórico - O Sinal GW150914

Selected for a Viewpoint in *Physics*

PRL **116,** 061102 (2016) PHYSICAL REVIEW LETTERS week ending 12 FEBRUARY 2016

Observation of Gravitational Waves from a Binary Black Hole Merger

B. P. Abbott *et al.*[*]

(LIGO Scientific Collaboration and Virgo Collaboration)

(Received 21 January 2016; published 11 February 2016)

On September 14, 2015 at 09:50:45 UTC the two detectors of the Laser Interferometer Gravitational-Wave Observatory simultaneously observed a transient gravitational-wave signal. The signal sweeps upwards in frequency from 35 to 250 Hz with a peak gravitational-wave strain of 1.0×10^{-21}. It matches the waveform predicted by general relativity for the inspiral and merger of a pair of black holes and the ringdown of the resulting single black hole. The signal was observed with a matched-filter signal-to-noise ratio of 24 and a false alarm rate estimated to be less than 1 event per 203 000 years, equivalent to a significance greater than 5.1σ. The source lies at a luminosity distance of 410^{+160}_{-180} Mpc corresponding to a redshift $z = 0.09^{+0.03}_{-0.04}$. In the source frame, the initial black hole masses are $36^{+5}_{-4}M_{\odot}$ $62^{+4}_{-4}M_{\odot}$, with $3.0^{+0.5}_{-0.5}M_{\odot}c^2$ radiated in gravitational waves. A These observations demonstrate the existence of binary stellar- detection of gravitational waves and the first observation of

DOI: 10.1103/PhysRevLett.116.061102

- DIVULGADORES: Kip Thorne (Caltech), France Córdova (NSF), Reiner Weiss (MIT), David Reitze (Caltech), Gabriela González (LSU).

Contexto Histórico - Observação de OGs e Rel. Numérica

- Forma de onda do sinal GW150914: 14 de setembro de 2015 9:50:45

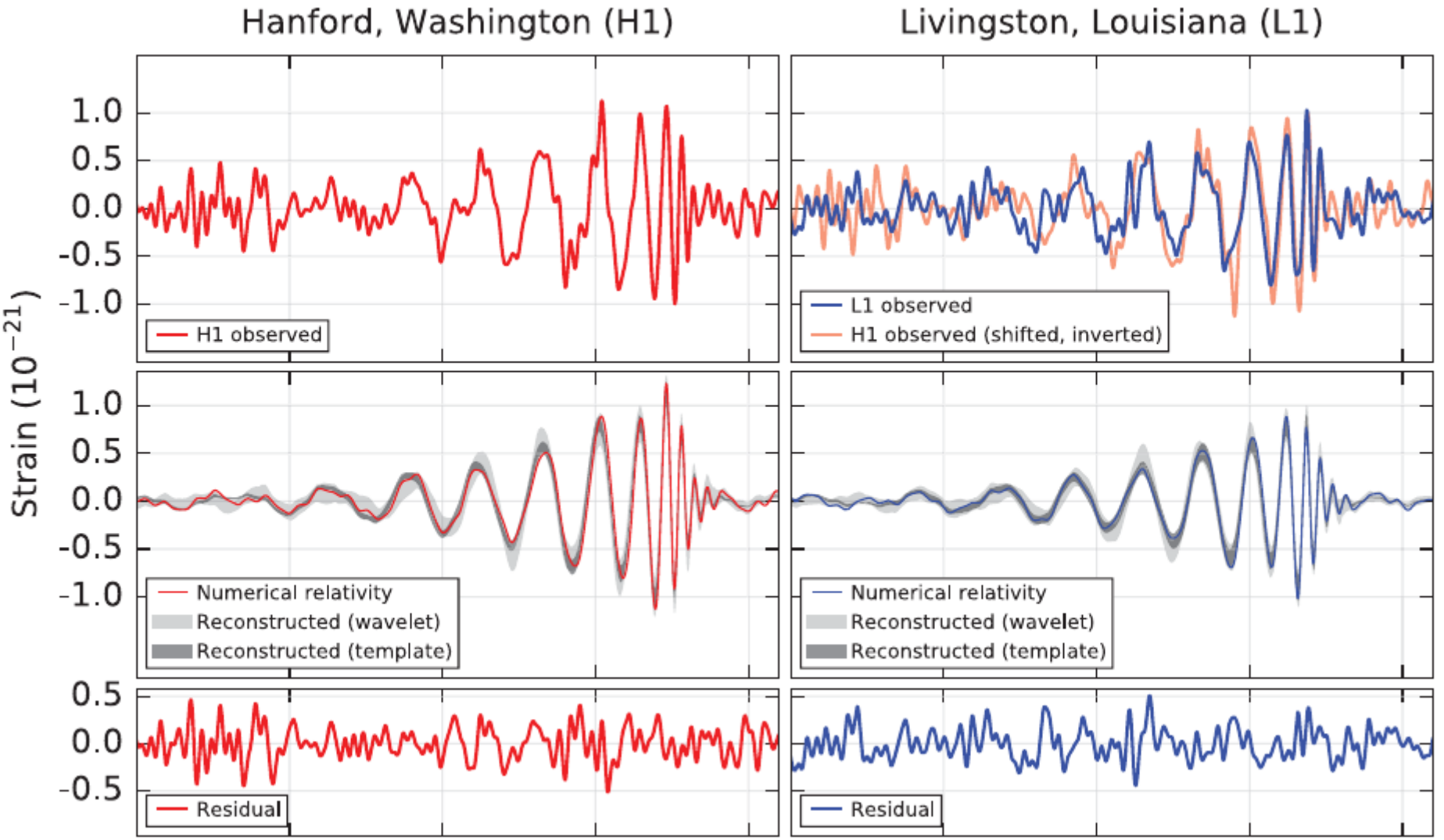

Contexto Histórico - Nobel de 2017

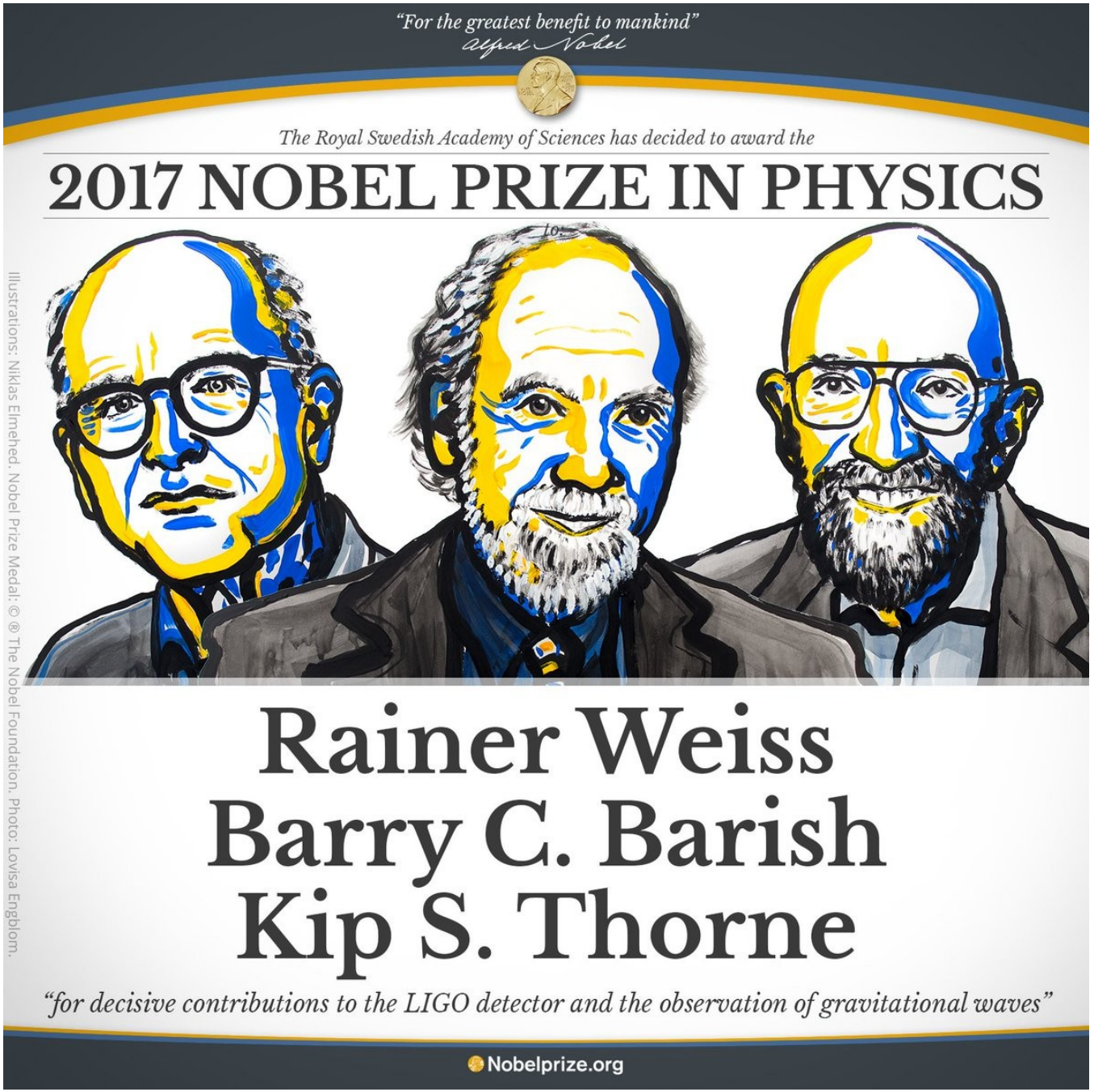

Contexto Histórico - Detecções seguintes

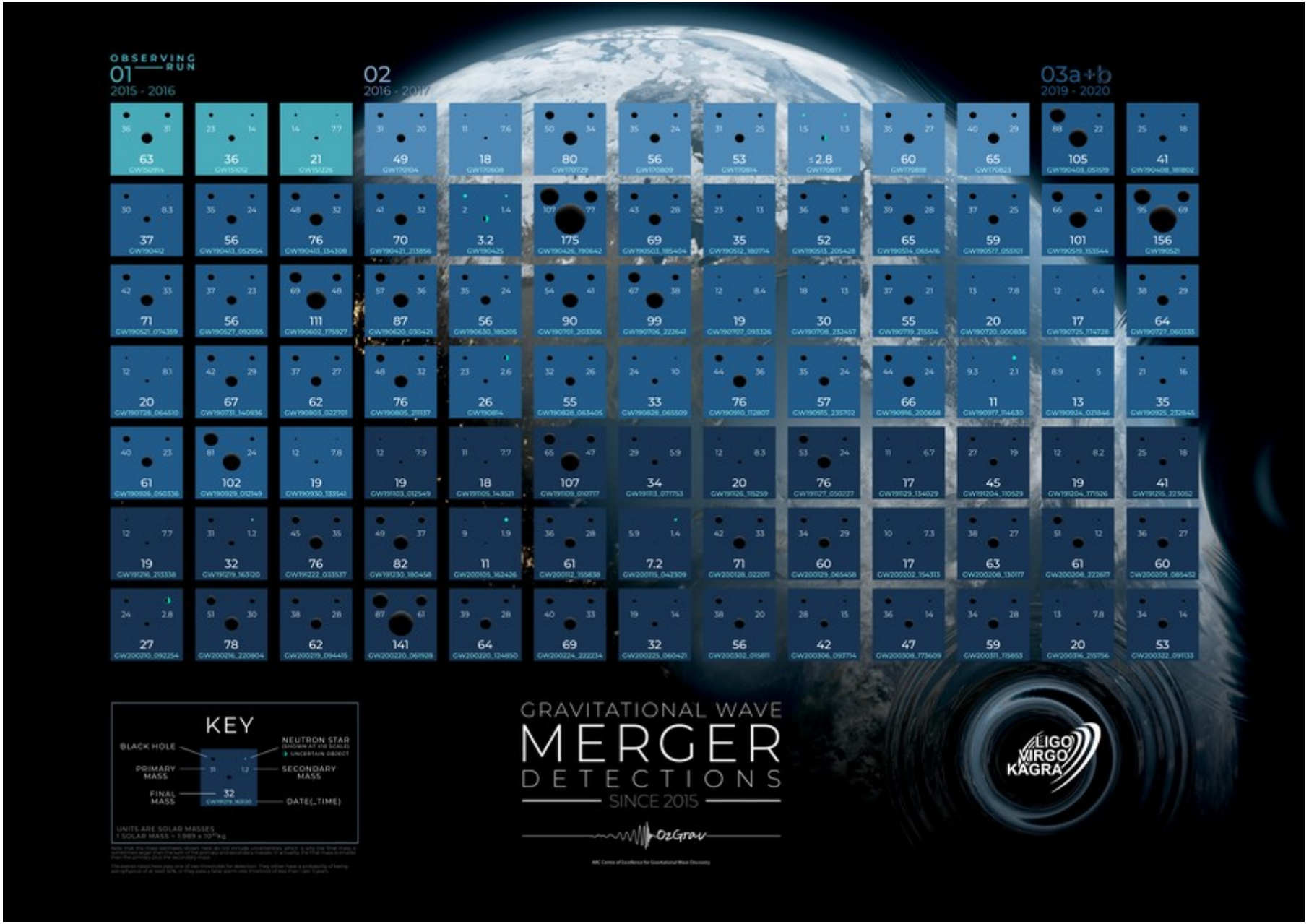

2
Formalismos Matemáticos

Formalismo ADM

ADM - Formulação 3+1

- Eventos altamente energéticos → Necessidade de incluir os graus de liberdade não-lineares.

$$G_{ab} \equiv {}^{(4)}R_{ab} - \frac{1}{2}\,{}^{(4)}R g_{ab} = 8\pi T_{ab}$$

ADM - Formulação 3+1

- Eventos altamente energéticos → Necessidade de incluir os graus de liberdade não-lineares.

$$G_{ab} \equiv {}^{(4)}R_{ab} - \frac{1}{2}\,{}^{(4)}R g_{ab} = 8\pi T_{ab}$$

- Método ADM (1959) → Formalismo hamiltoniano.

$$ds^2 = -\alpha^2 dt^2 + \gamma_{ij}(dx^i + \beta^i dt)(dx^j + \beta^j dt)$$

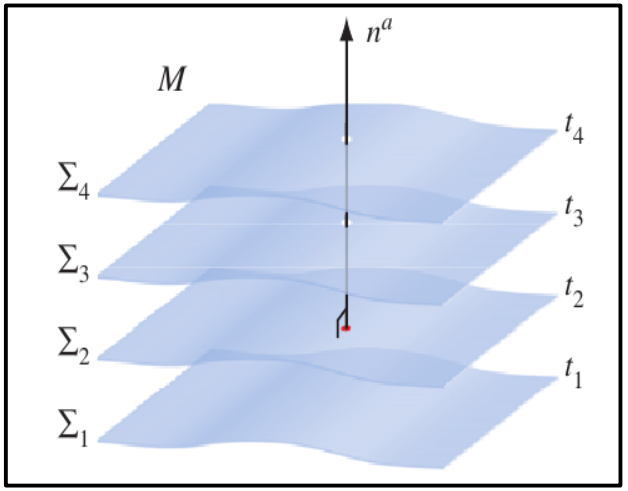

ADM - Formulação 3+1

- Eventos altamente energéticos → Necessidade de incluir os graus de liberdade não-lineares.

$$G_{ab} \equiv {}^{(4)}R_{ab} - \frac{1}{2}\,{}^{(4)}R g_{ab} = 8\pi T_{ab}$$

- Método ADM (1959) → Formalismo hamiltoniano.

$$ds^2 = -\alpha^2 dt^2 + \gamma_{ij}(dx^i + \beta^i dt)(dx^j + \beta^j dt)$$

- Curvatura extrínseca e matéria:

$$K_{ab} = -\frac{1}{2}\mathcal{L}_{\mathbf{n}}\gamma_{ab}, \quad \rho \equiv n_a n_b T^{ab}, \quad S_a \equiv -\gamma^b_{\ a} n^c T_{bc}$$

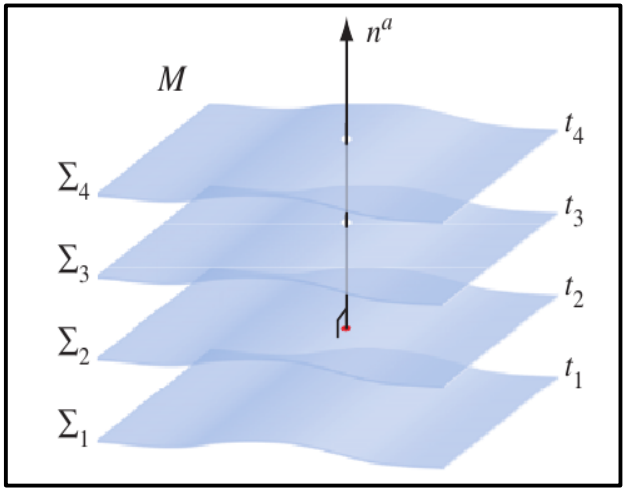

ADM - Formulação 3+1

- Eventos altamente energéticos → Necessidade de incluir os graus de liberdade não-lineares.

$$G_{ab} \equiv {}^{(4)}R_{ab} - \frac{1}{2}\,{}^{(4)}R g_{ab} = 8\pi T_{ab}$$

- Método ADM (1959) → Formalismo hamiltoniano.

$$ds^2 = -\alpha^2 dt^2 + \gamma_{ij}(dx^i + \beta^i dt)(dx^j + \beta^j dt)$$

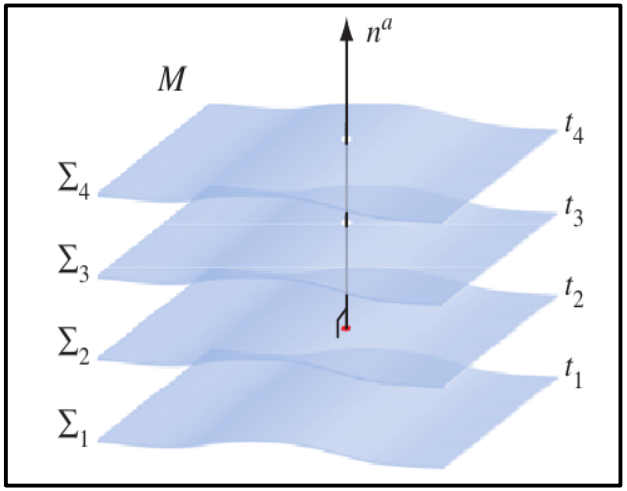

- Curvatura extrínseca e matéria:

$$K_{ab} = -\frac{1}{2}\mathcal{L}_{\mathbf{n}}\gamma_{ab}, \quad \rho \equiv n_a n_b T^{ab}, \quad S_a \equiv -\gamma^b_{\ a} n^c T_{bc}$$

- Equações de campo → Vínculos

$$R + K^2 - K_{ab}K^{ab} = 16\pi\rho$$

$$D_b K^b_{\ a} - D_a K = 8\pi S_a$$

ADM - Formulação 3+1

- Eventos altamente energéticos → Necessidade de incluir os graus de liberdade não-lineares.

$$G_{ab} \equiv {}^{(4)}R_{ab} - \frac{1}{2}\,{}^{(4)}R g_{ab} = 8\pi T_{ab}$$

- Método ADM (1959) → Formalismo hamiltoniano.

$$ds^2 = -\alpha^2 dt^2 + \gamma_{ij}(dx^i + \beta^i dt)(dx^j + \beta^j dt)$$

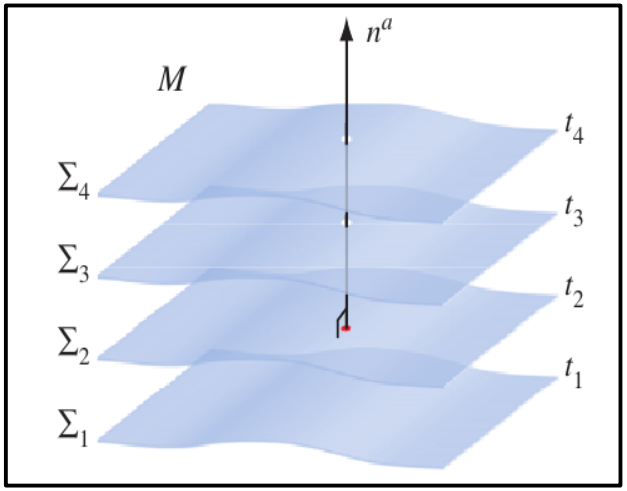

- Curvatura extrínseca e matéria:

$$K_{ab} = -\frac{1}{2}\mathcal{L}_{\mathbf{n}}\gamma_{ab}, \quad \rho \equiv n_a n_b T^{ab}, \quad S_a \equiv -\gamma^b_{\ a} n^c T_{bc}$$

- Equações de campo → Vínculos e dinâmica:

$$R + K^2 - K_{ab}K^{ab} = 16\pi\rho$$

$$D_b K^b_{\ a} - D_a K = 8\pi S_a$$

$$\partial_t K_{ij} = -D_i D_j \alpha + \alpha(R_{ij} - 2K_{ik}K^k_{\ j} + K K_{ij}) - 8\pi\alpha(S_{ij} - \tfrac{1}{2}\gamma_{ij}(S-\rho)) + \beta^k D_k K_{ij} + K_{ik} D_j \beta^k + K_{kj} D_i \beta^k,$$

$$\partial_t \gamma_{ij} = -2\alpha K_{ij} + D_i\beta_j + D_j\beta_i.$$

ADM - Escolha de gauge

Box 4.1 Lapse and shift conditions: a sampler

Geodesic slicing, or *Gaussian normal coordinates*, are defined by

$$\alpha = 1 \qquad \beta^i = 0. \tag{4.84}$$

Maximal slicing assumes $K = 0 = \partial_t K$, which results in the lapse equation

$$D^2\alpha = \alpha\Big(K_{ij}K^{ij} + 4\pi(\rho + S)\Big). \tag{4.85}$$

Sometimes maximal slicing is imposed "approximately" via a *K-driver*, as in equation (4.39). *Harmonic coordinates* satisfy

$${}^{(4)}\Gamma^a = 0, \tag{4.86}$$

which results in conditions (4.44) and (4.45) for the lapse and shift. An important variation is *1+log slicing*

$$(\partial_t - \beta^j\partial_j)\alpha = -2\alpha K. \tag{4.87}$$

For the *minimal distortion* gauge condition, the shift satisfies

$$(\Delta_L\beta)^i = 2A^{ij}D_j\alpha + \frac{4}{3}\alpha\gamma^{ij}D_jK + 16\pi\alpha S^i. \tag{4.88}$$

A related condition may be defined in terms of the "conformal connection functions" $\bar{\Gamma}^i$, which leads to the hyperbolic *Gamma-driver* condition for the shift,

$$\partial_t\beta^i = \frac{3}{4}B^i, \qquad \partial_t B^i = \partial_t\bar{\Gamma}^i - \eta B^i, \tag{4.89}$$

where η is a constant of order $1/(2M)$. Replacing the time derivatives ∂_t in equation (4.89) with advective derivatives $\partial_t - \beta^j\partial_j$ is one useful variation.

ADM - Dados Iniciais (puncturas)

- Formulação conforme da 3-métrica sem traço e curvatura.

$$\gamma_{ij} = \psi^4 \bar{\gamma}_{ij} \qquad A^{ij} = \psi^{-10} \bar{A}^{ij} \qquad K = \bar{K}$$

$$K_{ij} = A_{ij} + \frac{1}{3}\gamma_{ij} K$$

- Equações de vínculo:

$$8\bar{D}^2\psi - \psi \bar{R} - \frac{2}{3}\psi^5 K^2 + \psi^{-7}\bar{A}_{ij}\bar{A}^{ij} = -16\pi\psi^5\rho$$

$$\bar{D}_j \bar{A}^{ij} - \frac{2}{3}\psi^6 \bar{\gamma}^{ij}\bar{D}_j K = 8\pi\psi^{10} S^i$$

- Simetria temporal e conformalmente plano:

$$\beta^i = 0 \qquad K_{ij} = 0 = K \qquad \bar{R}_{ij} = \bar{R} = 0$$

$$\bar{D}^2\psi = 0$$

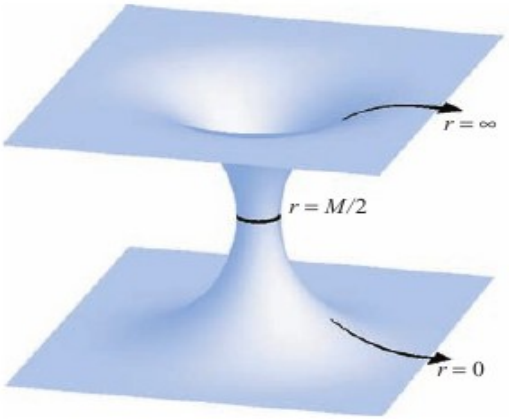

$$\psi = 1 + \frac{\mathcal{M}}{2r}$$

Um buraco negro

- Exemplo: Buraco negro de Schwarzschild.

$$\psi = 1 + \frac{\mathcal{M}}{2r}$$

$$dl^2 = \left(1 + \frac{M}{2r}\right)^4 \left(dr^2 + r^2(d\theta^2 + \sin^2\theta d\phi^2)\right)$$

Regime não-linear (campo forte) - Dados Iniciais (puncturas)

- Formulação conforme da 3-métrica sem traço e curvatura.

$$\gamma_{ij} = \psi^4 \bar{\gamma}_{ij} \qquad A^{ij} = \psi^{-10} \bar{A}^{ij} \qquad K = \bar{K}$$

$$K_{ij} = A_{ij} + \frac{1}{3}\gamma_{ij} K$$

- Equações de vínculo:

$$8\bar{D}^2\psi - \psi \bar{R} - \frac{2}{3}\psi^5 K^2 + \psi^{-7} \bar{A}_{ij}\bar{A}^{ij} = -16\pi\psi^5\rho$$

$$\bar{D}_j \bar{A}^{ij} - \frac{2}{3}\psi^6 \bar{\gamma}^{ij} \bar{D}_j K = 8\pi\psi^{10} S^i$$

- Simetria temporal e conformalmente plano:

$$\beta^i = 0 \qquad K_{ij} = 0 = K \qquad \bar{R}_{ij} = \bar{R} = 0$$

$$\bar{D}^2\psi = 0$$

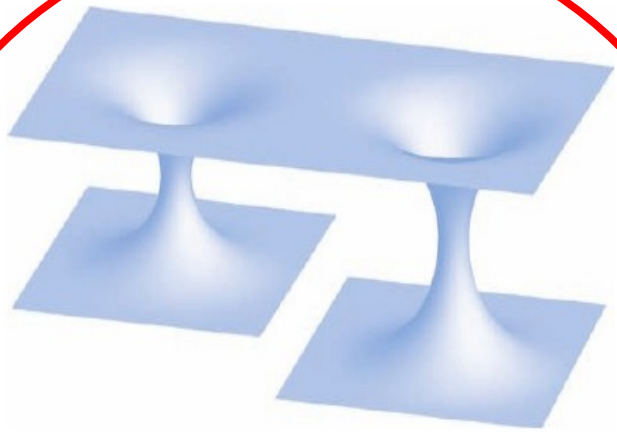

$$\psi = 1 + \frac{\mathcal{M}_1}{2r_1} + \frac{\mathcal{M}_2}{2r_2}$$

Dois buracos negros

- Exemplo: Buraco negro de Schwarzschild.

$$\psi = 1 + \frac{\mathcal{M}}{2r}$$

$$dl^2 = \left(1 + \frac{M}{2r}\right)^4 \left(dr^2 + r^2(d\theta^2 + \sin^2\theta d\phi^2)\right)$$

Regime não-linear (campo forte) - Localizando Buracos Negros

- Projeção em uma superfície 2D:

$$m_{ab} = g_{ab} + k_a l_b + l_a k_b$$

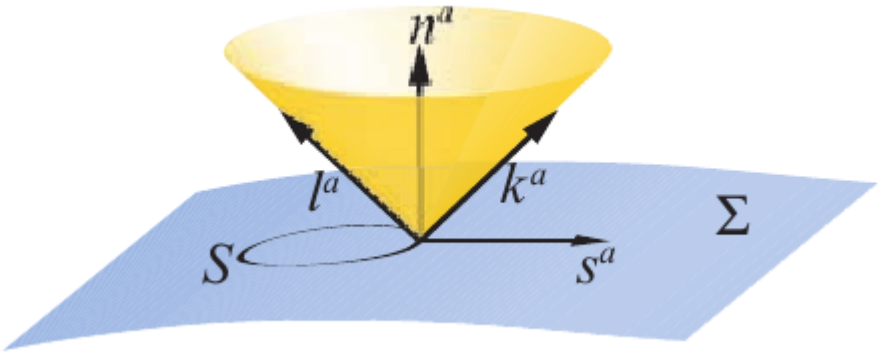

- Expansão de geodésicas nulas:

$$\Theta = m^{ab} \nabla_a k_b$$

- Superfície aprisionada → Superfície S onde raios não escapam (expansão nula).

$$\Theta = 0$$

- Região de aprisionamento → Contorno de S.
- HORIZONTE APARENTE → conjunto de R.A.'s.

- Exemplo: Métrica de Vaidya (avançada):

$$ds^2 = -f\, dv^2 + 2\, dv\, dr + r^2\, d\Omega^2$$

$$f = 1 - \frac{2m(v)}{r}$$

$$\Theta = 0 \longrightarrow r - 2m(v) = 0$$

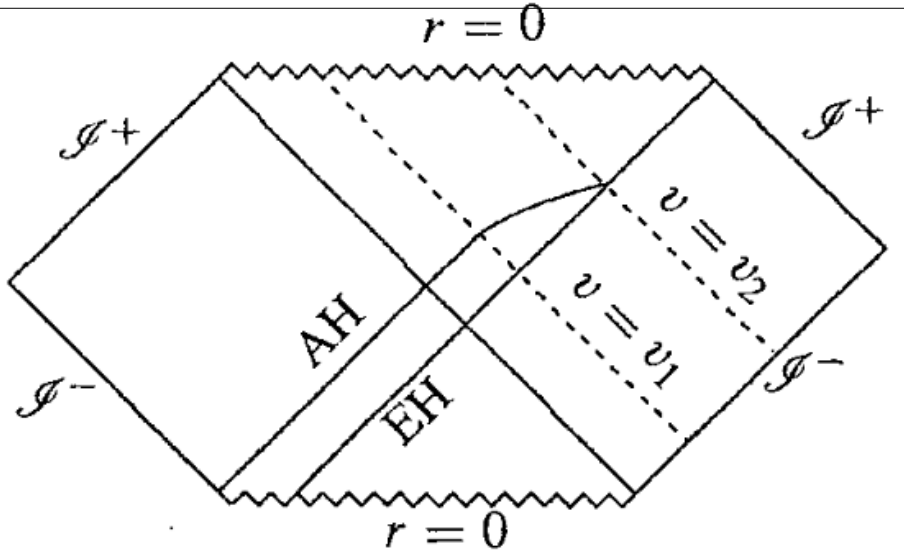

Hiperbolicidade

ADM - Hiperbolicidade

- Ex: Equações de Maxwell:

$$\partial_t A_i = -E_i - D_i \Phi$$

$$\partial_t E_i = -D^j D_j A_i + D_i D^j A_j - 4\pi j_i$$

ADM - Hiperbolicidade

- Ex: Equações de Maxwell:

$$\partial_t A_i = -E_i - D_i \Phi$$
$$\partial_t E_i = -D^j D_j A_i + D_i D^j A_j - 4\pi j_i$$

- Equação tipo onda para os potenciais:

$$-\partial_t^2 A_i + D^j D_j A_i - D_i D^j A_j = D_i \partial_t \Phi - 4\pi j_i$$

ADM - Hiperbolicidade

- Ex: Equações de Maxwell:

$$\partial_t A_i = -E_i - D_i \Phi$$
$$\partial_t E_i = -D^j D_j A_i + D_i D^j A_j - 4\pi j_i$$

- Equação tipo onda para os potenciais:

$$-\partial_t^2 A_i + D^j D_j A_i - D_i D^j A_j = D_i \partial_t \Phi - 4\pi j_i$$

- Caso gravitacional:

$$\partial_t \gamma_{ij} = -2\alpha K_{ij} + D_i \beta_j + D_j \beta_i$$

$$\partial_t K_{ij} = \alpha(R_{ij} - 2K_{ik}K^k_{\ j} + K K_{ij}) - D_i D_j \alpha - 8\pi\alpha(S_{ij} - \tfrac{1}{2}\gamma_{ij}(S-\rho)) + \beta^k \partial_k K_{ij} + K_{ik}\partial_j \beta^k + K_{kj}\partial_i \beta^k.$$

$$R_{ij} = \frac{1}{2}\gamma^{kl}\left(\partial_l \partial_i \gamma_{kj} + \partial_j \partial_k \gamma_{il} - \partial_j \partial_i \gamma_{kl} - \partial_l \partial_k \gamma_{ij}\right) + \gamma^{kl}\left(\Gamma^m_{il}\Gamma_{mkj} - \Gamma^m_{ij}\Gamma_{mkl}\right)$$

ADM - Hiperbolicidade

- Ex: Equações de Maxwell:

$$\partial_t A_i = -E_i - D_i \Phi$$
$$\partial_t E_i = -D^j D_j A_i + D_i D^j A_j - 4\pi j_i$$

- Equação tipo onda para os potenciais:

$$-\partial_t^2 A_i + D^j D_j A_i - D_i D^j A_j = D_i \partial_t \Phi - 4\pi j_i$$

- Caso gravitacional:

TERMOS QUE GERAM A HIPERBOLICIDADE FRACA NO SISTEMA DE EQUAÇÕES!

$$\partial_t \gamma_{ij} = -2\alpha K_{ij} + D_i \beta_j + D_j \beta_i$$

$$\partial_t K_{ij} = \alpha(R_{ij} - 2K_{ik}K^k{}_j + K K_{ij}) - D_i D_j \alpha - 8\pi\alpha(S_{ij} - \tfrac{1}{2}\gamma_{ij}(S-\rho)) + \beta^k \partial_k K_{ij} + K_{ik}\partial_j \beta^k + K_{kj}\partial_i \beta^k.$$

$$R_{ij} = \frac{1}{2}\gamma^{kl}\left(\partial_l\partial_i\gamma_{kj} + \partial_j\partial_k\gamma_{il} - \partial_j\partial_i\gamma_{kl} - \partial_l\partial_k\gamma_{ij}\right) + \gamma^{kl}\left(\Gamma^m_{il}\Gamma_{mkj} - \Gamma^m_{ij}\Gamma_{mkl}\right)$$

Formalismo BSSN

Formalismo BSSN - Vínculos

- Formalismo Baumgarte-Shapiro-Shibata-Nakamura → Instaurar a hiperbolicidade forte nas equações de campo:

Introdução de novas variáveis:

$$\bar{\gamma}_{ij} = e^{-4\phi}\gamma_{ij} \qquad \tilde{A}_{ij} = e^{-4\phi}A_{ij}$$

$$\psi = e^{\phi} \qquad \bar{\Gamma}^{i} \equiv \bar{\gamma}^{jk}\bar{\Gamma}^{i}_{jk}$$

- Equações de vínculo BSSN:

Vínculo Hamiltoniano:

$$0 = \mathcal{H} = \bar{\gamma}^{ij}\bar{D}_i\bar{D}_j e^{\phi} - \frac{e^{\phi}}{8}\bar{R} + \frac{e^{5\phi}}{8}\tilde{A}_{ij}\tilde{A}^{ij} - \frac{e^{5\phi}}{12}K^2 + 2\pi e^{5\phi}\rho$$

Vínculo de Momento:

$$0 = \mathcal{M}^{i} = \bar{D}_j(e^{6\phi}\tilde{A}^{ji}) - \frac{2}{3}e^{6\phi}\bar{D}^{i}K - 8\pi e^{6\phi}S^{i}$$

Formalismo BSSN - Dinâmica

- Equações dinâmicas BSSN:

$$\partial_t \phi = -\frac{1}{6}\alpha K + \beta^i \partial_i \phi + \frac{1}{6}\partial_i \beta^i$$

$$\partial_t \bar{\gamma}_{ij} = -2\alpha \tilde{A}_{ij} + \beta^k \partial_k \bar{\gamma}_{ij} + \bar{\gamma}_{ik}\partial_j \beta^k + \bar{\gamma}_{kj}\partial_i \beta^k - \frac{2}{3}\bar{\gamma}_{ij}\partial_k \beta^k$$

$$\partial_t K = -\gamma^{ij} D_j D_i \alpha + \alpha(\tilde{A}_{ij}\tilde{A}^{ij} + \frac{1}{3}K^2) + 4\pi\alpha(\rho + S) + \beta^i \partial_i K$$

$$\partial_t \tilde{A}_{ij} = e^{-4\phi}\left(-(D_i D_j \alpha)^{TF} + \alpha(R_{ij}^{TF} - 8\pi S_{ij}^{TF})\right) + \alpha(K\tilde{A}_{ij} - 2\tilde{A}_{il}\tilde{A}^l{}_j) + \beta^k \partial_k \tilde{A}_{ij} + \tilde{A}_{ik}\partial_j \beta^k + \tilde{A}_{kj}\partial_i \beta^k - \frac{2}{3}\tilde{A}_{ij}\partial_k \beta^k.$$

$$\partial_t \bar{\Gamma}^i = -2\tilde{A}^{ij}\partial_j \alpha + 2\alpha\left(\bar{\Gamma}^i_{jk}\tilde{A}^{kj} - \frac{2}{3}\bar{\gamma}^{ij}\partial_j K - 8\pi\bar{\gamma}^{ij}S_j + 6\tilde{A}^{ij}\partial_j \phi\right) + \beta^j \partial_j \bar{\Gamma}^i - \bar{\Gamma}^j \partial_j \beta^i + \frac{2}{3}\bar{\Gamma}^i \partial_j \beta^j + \frac{1}{3}\bar{\gamma}^{li}\partial_l \partial_j \beta^j + \bar{\gamma}^{lj}\partial_j \partial_l \beta^i.$$

$$\bar{R}_{ij} = -\frac{1}{2}\bar{\gamma}^{lm}\partial_m \partial_l \bar{\gamma}_{ij} + \bar{\gamma}_{k(i}\partial_{j)}\bar{\Gamma}^k + \bar{\Gamma}^k \bar{\Gamma}_{(ij)k} + \bar{\gamma}^{lm}\left(2\bar{\Gamma}^k_{l(i}\bar{\Gamma}_{j)km} + \bar{\Gamma}^k_{im}\bar{\Gamma}_{klj}\right)$$

Formalismo BSSN - ADM versus BSSN

- Evolução da componente zz (cartesianas) da curvatura extrínseca:

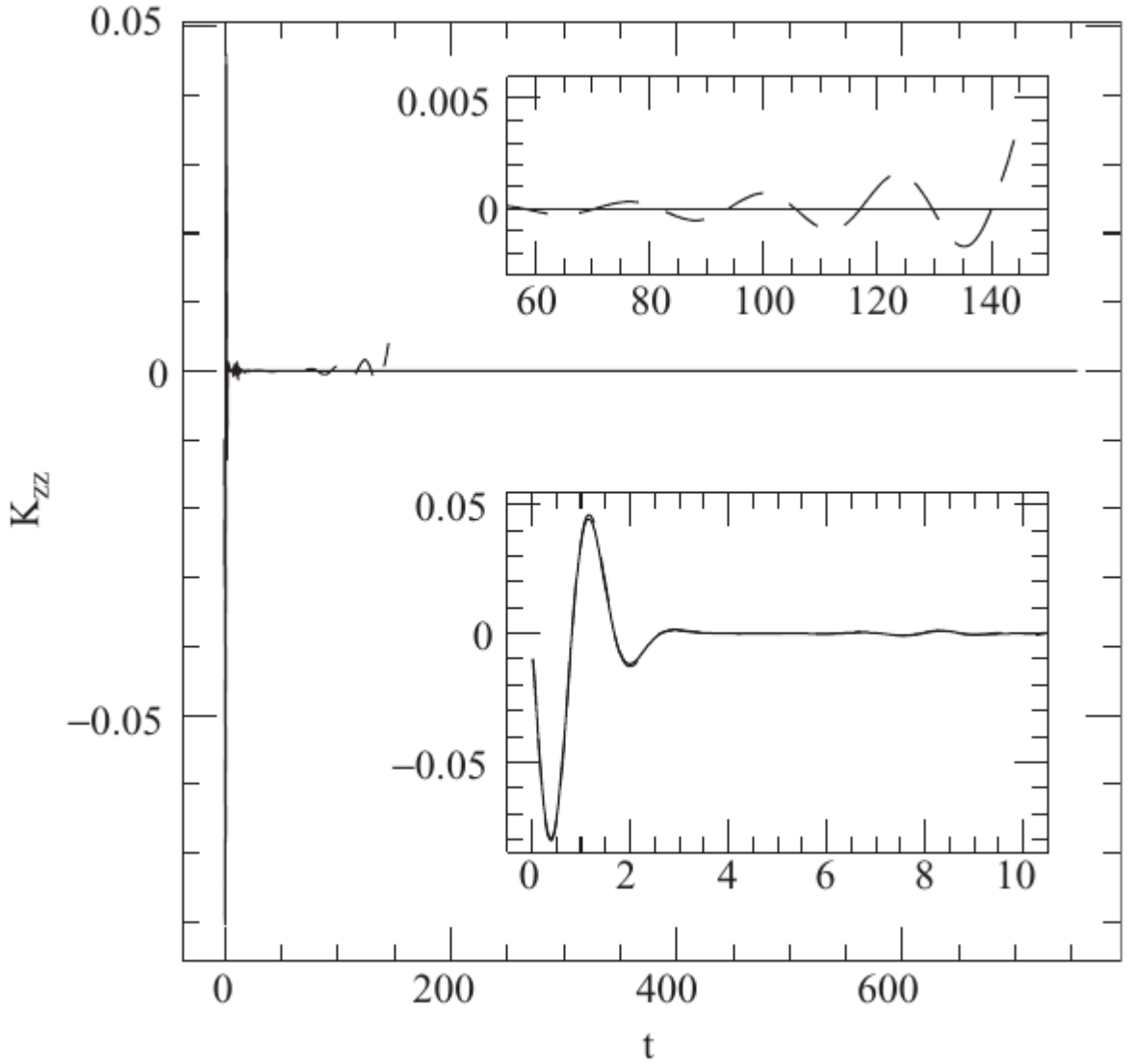

INSTAURAÇÃO DA HIPERBOLICIDADE FORTE TORNA O SISTEMA ESTÁVEL!!!

Formalismo G-BSSN

Formalismo BSSN - Vínculos

- Formalismo Baumgarte-Shapiro-Shibata-Nakamura → Instaurar a hiperbolicidade forte nas equações de campo:

Introdução de novas variáveis:

$$\bar{\gamma}_{ij} = e^{-4\phi}\gamma_{ij} \qquad \tilde{A}_{ij} = e^{-4\phi}A_{ij}$$

$$\psi = e^{\phi} \qquad \bar{\Gamma}^{i} \equiv \bar{\gamma}^{jk}\bar{\Gamma}^{i}_{jk}$$

- Equações de vínculo BSSN:

Vínculo Hamiltoniano:

$$0 = \mathcal{H} = \bar{\gamma}^{ij}\bar{D}_i\bar{D}_j e^{\phi} - \frac{e^{\phi}}{8}\bar{R} + \frac{e^{5\phi}}{8}\tilde{A}_{ij}\tilde{A}^{ij} - \frac{e^{5\phi}}{12}K^2 + 2\pi e^{5\phi}\rho$$

Vínculo de Momento:

$$0 = \mathcal{M}^{i} = \bar{D}_j(e^{6\phi}\tilde{A}^{ji}) - \frac{2}{3}e^{6\phi}\bar{D}^{i}K - 8\pi e^{6\phi}S^{i}$$

Formalismo BSSN - Vínculos

- Formalismo Baumgarte-Shapiro-Shibata-Nakamura → Instaurar a hiperbolicidade forte nas equações de campo:

Introdução de novas variáveis:

$$\bar{\gamma}_{ij} = e^{-4\phi}\gamma_{ij} \qquad \tilde{A}_{ij} = e^{-4\phi}A_{ij}$$

$$\psi = e^{\phi} \qquad \bar{\Gamma}^i \equiv \bar{\gamma}^{jk}\bar{\Gamma}^i_{jk}$$

Not a tensor!

- Equações de vínculo BSSN:

Vínculo Hamiltoniano:

$$0 = \mathcal{H} = \bar{\gamma}^{ij}\bar{D}_i\bar{D}_j e^{\phi} - \frac{e^{\phi}}{8}\bar{R} + \frac{e^{5\phi}}{8}\tilde{A}_{ij}\tilde{A}^{ij} - \frac{e^{5\phi}}{12}K^2 + 2\pi e^{5\phi}\rho$$

Vínculo de Momento:

$$0 = \mathcal{M}^i = \bar{D}_j(e^{6\phi}\tilde{A}^{ji}) - \frac{2}{3}e^{6\phi}\bar{D}^i K - 8\pi e^{6\phi}S^i$$

Generalized BSSN - Coordenadas curvilíneas

- Nova variável covariante:

$$\tilde{\Lambda}^k \equiv \tilde{\gamma}^{ij}(\tilde{\Gamma}^k_{ij} - \mathring{\Gamma}^k_{ij}) = \tilde{\Gamma}^k - \mathring{\Gamma}^k_{ij}\tilde{\gamma}^{ij}$$

Brown, PRD (2009).

- Novo sistema de equações:

$$\partial_\perp \phi = -\frac{1}{6}\alpha K + \sigma\frac{1}{6}\tilde{D}_k\beta^k,$$

$$\partial_\perp \tilde{\gamma}_{ij} = -2\alpha\tilde{A}_{ij} - \sigma\frac{2}{3}\tilde{A}_{ij}\tilde{D}_k\beta^k,$$

$$\partial_\perp K = -\gamma^{ij}D_jD_i\alpha + \alpha\left(\tilde{A}_{ij}\tilde{A}^{ij} + \frac{1}{3}K^2\right) + 4\pi(\rho + S),$$

$$\partial_\perp \tilde{A}_{ij} = e^{-4\phi}[-D_iD_j\alpha + \alpha(R_{ij} - 8\pi S_{ij})]^{\mathrm{TF}} + \alpha(K\tilde{A}_{ij} - 2\tilde{A}_{il}\tilde{A}^l{}_j) - \sigma\frac{2}{3}\tilde{A}_{ij}\tilde{D}_k\beta^k,$$

$$\partial_t\tilde{\Lambda}^k = \partial_t\tilde{\Gamma}^k - \mathring{\Gamma}^k_{ij}\partial_t\tilde{\gamma}^{ij},$$

$$\partial_\perp \equiv \partial_t - \mathcal{L}_{\vec{\beta}}$$

$$\rho = n_\mu n_\nu T^{\mu\nu},$$

$$S = \gamma^{ij}S_{ij},$$

$$S^i = -\gamma^{ij}n^\mu T_{\mu j},$$

$$S_{ij} = \gamma_{i\mu}\gamma_{i\nu}T^{\mu\nu},$$

Generalized BSSN - Coordenadas curvilíneas

- Vínculos hamiltoniano e de momento:

$$\mathcal{H} \equiv \tilde{\gamma}^{ij}\tilde{D}_i\tilde{D}_j e^{\phi} - \frac{e^{\phi}}{8}\tilde{R} + \frac{e^{5\phi}}{8}\tilde{A}^{ij}\tilde{A}_{ij} - \frac{e^{5\phi}}{12}K^2 + 2\pi e^{5\phi}\rho = 0,$$

$$\mathcal{M}^i \equiv \tilde{D}_j(e^{6\phi}\tilde{A}^{ji}) - \frac{2}{3}e^{6\phi}\tilde{D}^i K - 8\pi e^{6\phi}S^i = 0.$$

- Gauge log+1 e gamma driver:

$$\partial_t \alpha = -2\alpha k.$$

$$\partial_t \beta^i = \mu\tilde{\Lambda}^i - \eta\beta^i.$$

- Objetos dentro de simetria esférica:

$$\tilde{\gamma}_{ij} = \begin{pmatrix} \tilde{\gamma}_{rr}(t,r) & 0 & 0 \\ 0 & r^2\tilde{\gamma}_{\theta\theta}(t,r) & 0 \\ 0 & 0 & r^2\tilde{\gamma}_{\theta\theta}(t,r)\sin^2\theta \end{pmatrix}.$$

3
Métodos Numéricos

Diferençaas Finitas

Métodos Numéricos - Diferenças Finitas

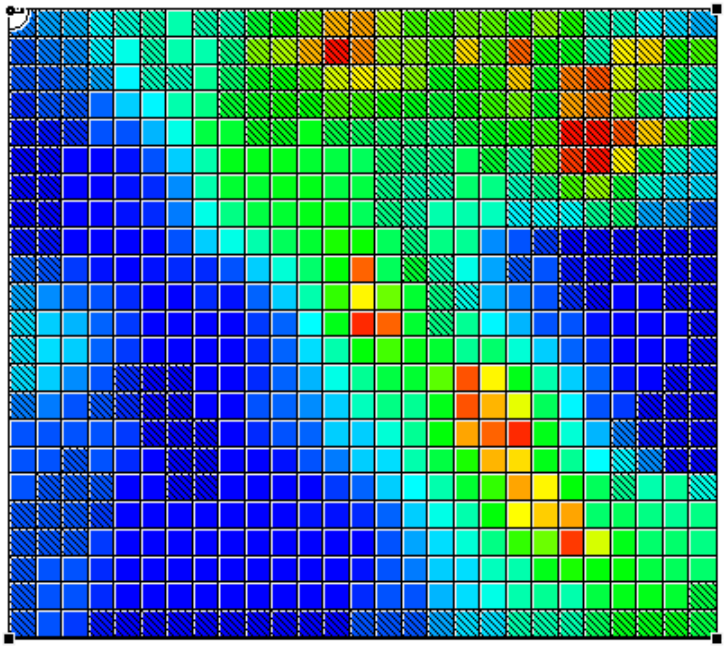

- Discretização do espaço-tempo → Grid.
- Expansão de Taylor a partir do ponto inicial do grid → Eqs. Discretizadas.

- Ex: Equação do calor 1D:

$$\partial_t \phi - \kappa \partial_x^2 \phi = 0$$

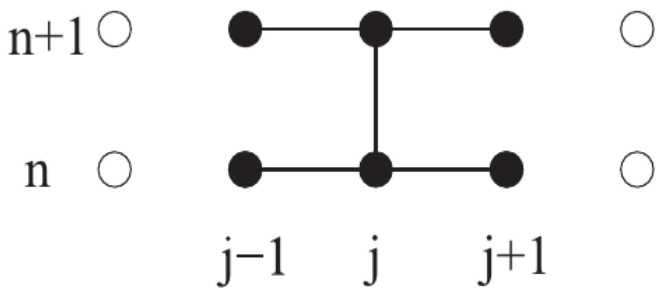

$$\phi_j^{n+1} = \phi_j^n + \frac{\kappa \Delta t}{2(\Delta x)^2}\left((\phi_{j+1}^{n+1} - 2\phi_j^{n+1} + \phi_{j-1}^{n+1}) + (\phi_{j+1}^{n} - 2\phi_j^{n} + \phi_{j-1}^{n})\right)$$

Método de Cranck-Nicholson

Métodos Numéricos - AMR

- Refinamento de malha adaptada (AMR): Função lapso para duas estrelas de nêutron (Pretorius)

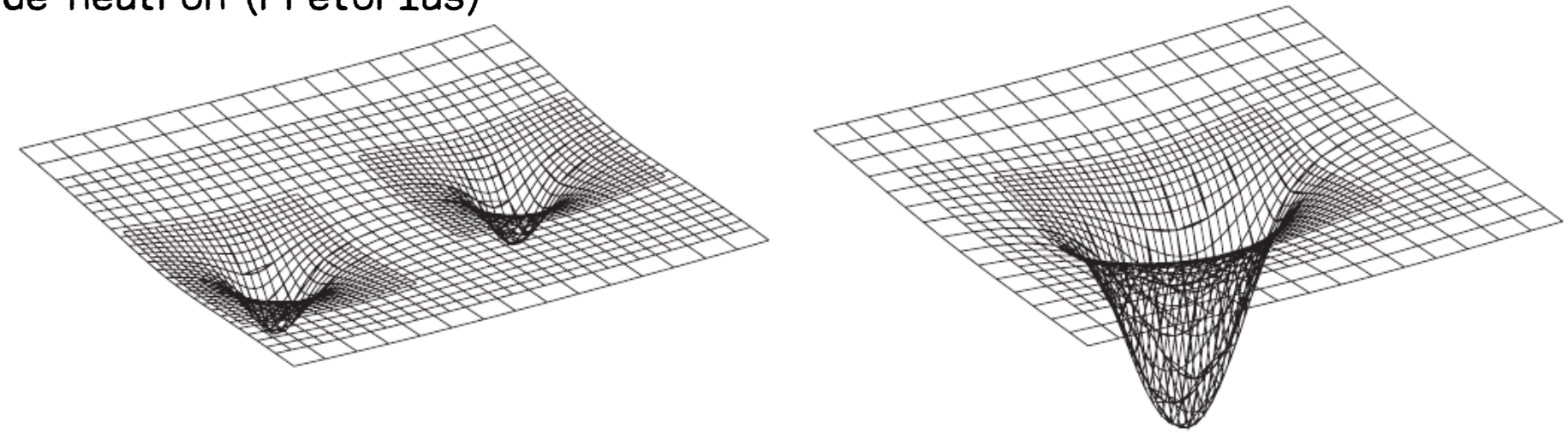

- CARPET: Software AMR (carpetcode.org)

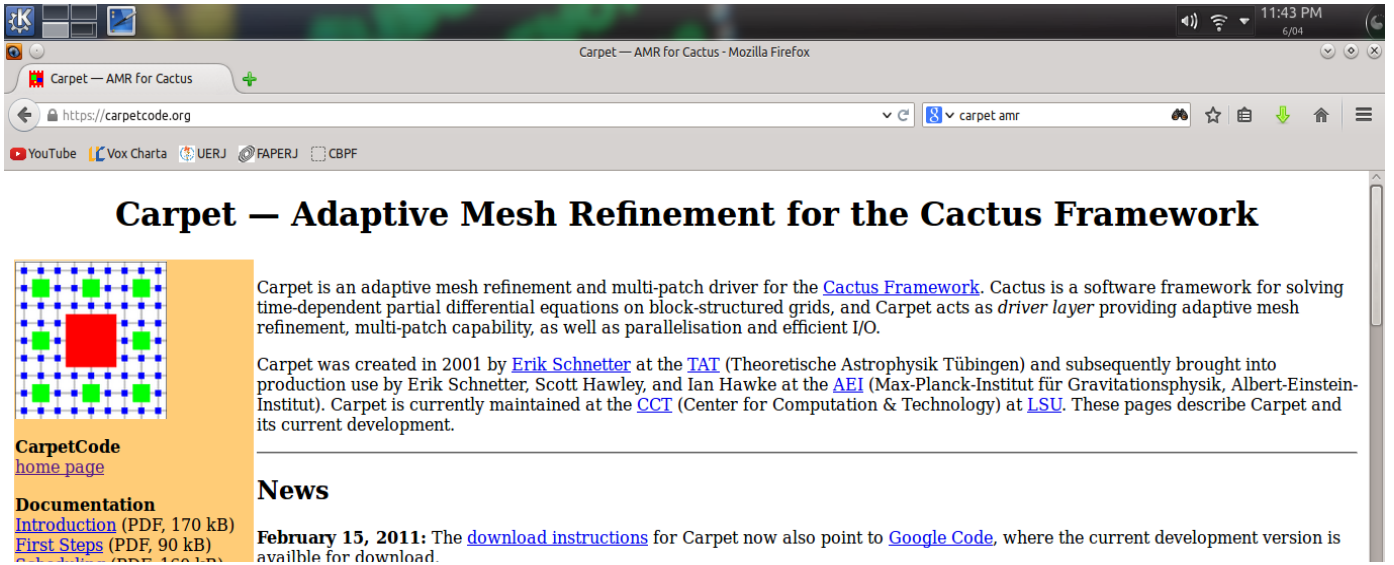

BSSN + Diferenças Finitas - Einstein Toolkit

Einstein Toolkit → Repositório de ferramentas computacionais para problemas de Astrofísica Relativística. 247 instituições, 353 membros.

einsteintoolkit.org

einstein toolkit

Home About Download Documentation Help! Contribute Gallery

The Einstein Toolkit

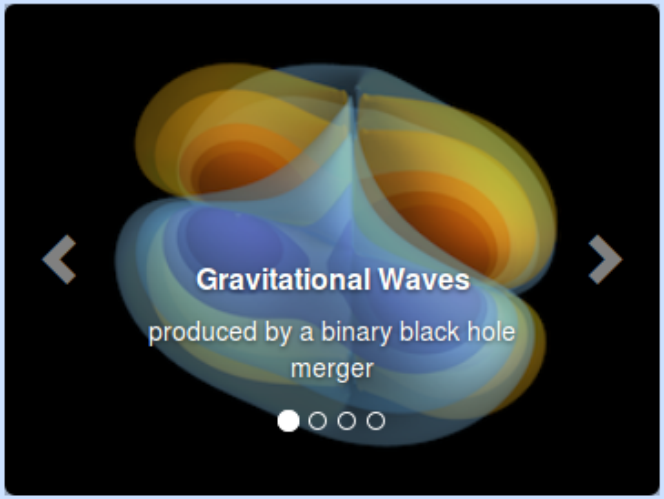

Gallery

Einstein Toolkit School and Workshop

Thank you all for making the North American Einstein Toolkit School and Workshop at NCSA, at the University of Illinois at Urbana-Champaign from July 31 to August 4 2017 a success.

This meeting was open to anyone interested in numerical relativity and computational astrophysics and cosmology and in particular to Einstein toolkit users.

The first three days were dedicated to a school useful for new users of the Einstein Toolkit followed by a two day long workshop open to developers interested in the Einstein Toolkit.

Watch the school lectures on YouTube or visit the conference website for further information in the Instructions tab.

More information

About

The Einstein Toolkit is a community-driven software platform of core computational tools to advance and support research in relativistic astrophysics and gravitational physics.

About

Documentation

A lot of the documentation within the Einstein Toolkit is generated from comments in the source code, and more can be found on the Einstein Toolkit Wiki or other documents. We provide links to guides, tutorials and references.

Métodos Espectrais

Métodos Espectrais

- Expansão espectral no espaço de Hilbert L2(a,b):

$$f(x) = \sum_{n=0}^{\infty} f_n^{\phi} \phi_n(x)$$

$$f_n^{\phi} = \frac{(\phi_n, f)_{\phi}}{(\phi_n, \phi_n)_{\phi}} \equiv \langle \phi_n | f \rangle$$

- Equação geral (linear e não linear):

$$Lu(x_i) = f(x_i), \qquad i = 0, \ldots, N-1.$$

- Equação espectral (coeficientes espectrais)

$$\sum_n \langle \psi_i | L\phi_n \rangle u_n^{\phi} = \sum_n \langle \psi_i | \phi_n \rangle f_n^{\phi}, \qquad i = 0, \ldots, N-1.$$

Método Pseudoespectral

- Exemplo:

$$u_{xx} - (x^6 + 3x^2)u = 0$$

$$u(-1) = u(1) = 1$$

- Solução exata e *ansatz*:

$$u(x) = \exp([x^4 - 1]/4)$$

$$u_2 = 1 + (1 - x^2)(a_0 + a_1 x + a_2 x^2)$$

- Definição de Resíduo:

$$R(x; a_0, a_1, a_2) = u_{2,xx} - (x^6 + 3x^2)u_2$$

- Resíduo com a solução aproximada:

$$\begin{aligned} R \quad = \quad & (2a_2 + 2a_0) - 6a_1 x - (3 + 3a_0 + 12a_2)x^2 - 3a_1 x^3 + 3(a_0 - a_2)x^4 \\ & +3a_1 x^5 + (-1 - a_0 + 3a_2)x^6 - a_1 x^7 + (a_0 - a2)x^8 + a_1 x^9 + 10a_2 x^{10} \end{aligned}$$

Método Pseudoespectral

- Pontos de colocação e obtenção dos coef. espectrais:

$$x_i = (-1/2, 0, 1/2)$$

$$\begin{aligned} eq1 &= -\frac{659}{256}a_0 + \frac{1683}{512}a_1 - \frac{1171}{1024}a_2 - \frac{49}{64} \\ eq2 &= -2(a_0 - a_2) \\ eq3 &= -\frac{659}{256}a_0 - \frac{1683}{512}a_1 - \frac{1171}{1024}a_2 - \frac{49}{64} \end{aligned}$$

$$a_0 = -\frac{784}{3807}, \qquad a_1 = 0, \qquad a_2 = a_0$$

Solução exata
x
aproximada

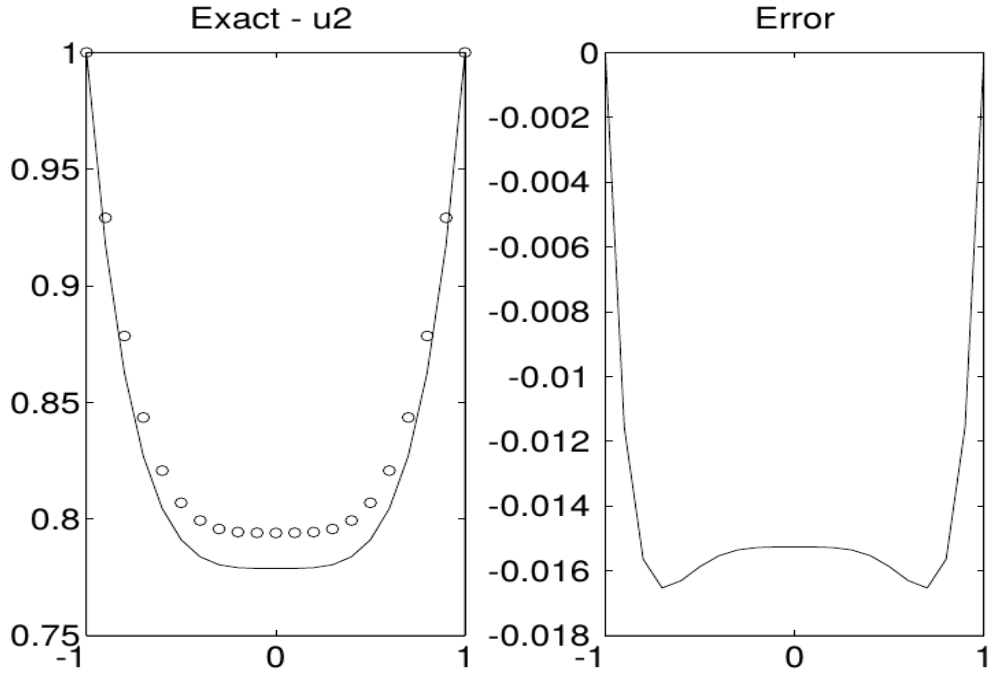

Spectral Einstein Code

Introduction Contributors Publications External Software

Introduction

The Spectral Einstein Code (SpEC) is a flexible infrastructure for solving partial differential equations using multi-domain spectral methods. While SpEC was primarily designed for fully general-relativistic compact object simulations, it can be applied to a wide range of hyperbolic and elliptic equations. Some of its features are:

- A flexible domain decomposition supporting individual subdomains (cells, elements) of various topologies, e.g. blocks, spheres, cylinders, and any combination thereof. Subdomains can touch or overlap.
- Solves hyperbolic and elliptic PDEs.
- Interfaces to the visualization software ParaView and VisIt.

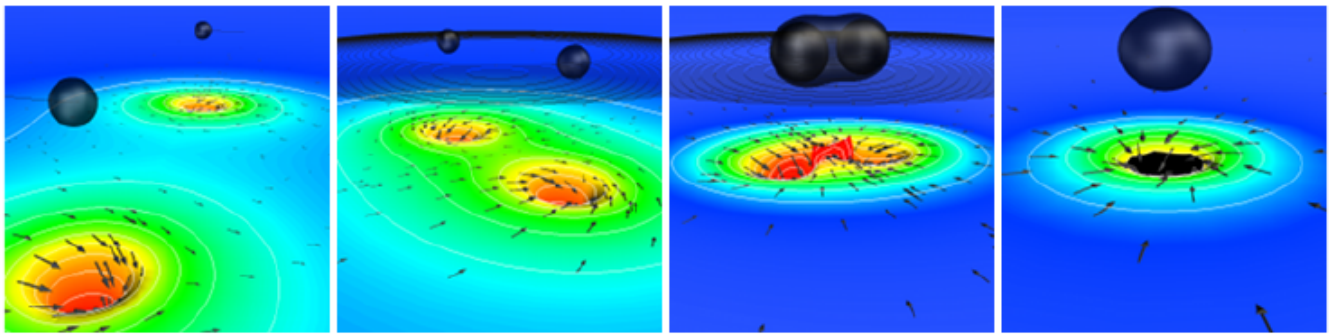

SpEC simulation of inspiral and merger of two black holes

The main application area of SpEC lies in simulating compact binary objects. Specifically, it is one of the most accurate and efficient codes to compute the gravitational waveforms for inspiraling and coalescing binary black holes.

4

NumRel - UERJ

Sobre o Grupo

Motivação

- Código próprio - NumRel/UERJ.
- Plataforma Open Source - GitHub.
- User friendly
- Métodos Espectrais + Formalismo G-BSSN

Gravitação
Cosmologia
UERJ

open source

GitHub

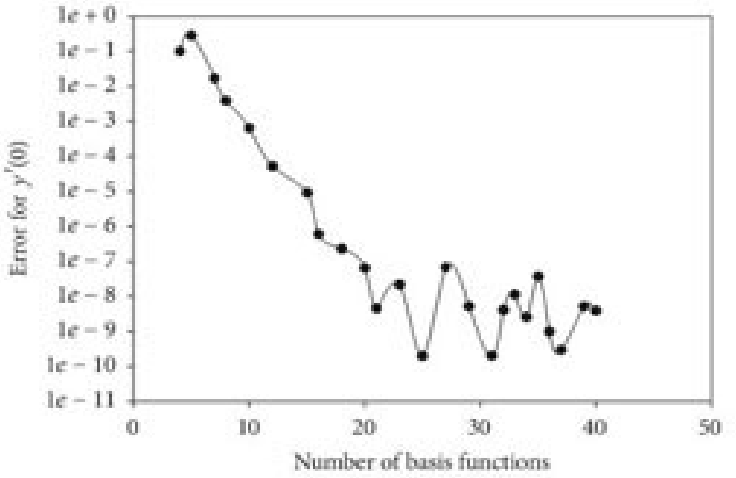

FIGURE 3: Detailed presentation of the convergence rate of the initial slope $y'(0)$ for an exponential basis set defined with the following parameters: $s = 5$, $d_s = -4$, and $d_l = 2$.

R. Jovanovic, JAM (2014)

Grupo NumRel-UERJ - 2022

Membros:

- Henrique de Oliveira
- Rafael Aranha
- Mariana Alcoforado (Pós-Doc)

Colaboradores:

- Willians Barreto (ULA/UFABC)

Capacidade computacional

- 1 máquina com processadores i7 - 8 núcleos de 3.6 GHz - 64Gb RAM.
- 1 máquina com processadores i7 - 6 núcleos de 3.6 GHz - 32Gb RAM.
- 1 máquina com processadores i7 - 4 núcleos de 3.6 GHz - 32Gb RAM.

Software - Repositórios (Initial status)

- Protótipos e oficiais em Fortran, Python e C++ (not yet!).
- Paralelização (MPI).
- Construídos a partir de aplicações mais simples (bottom-up).
- Visualização - GNUPlot, Matplotlib.
- Repositório GitHub.

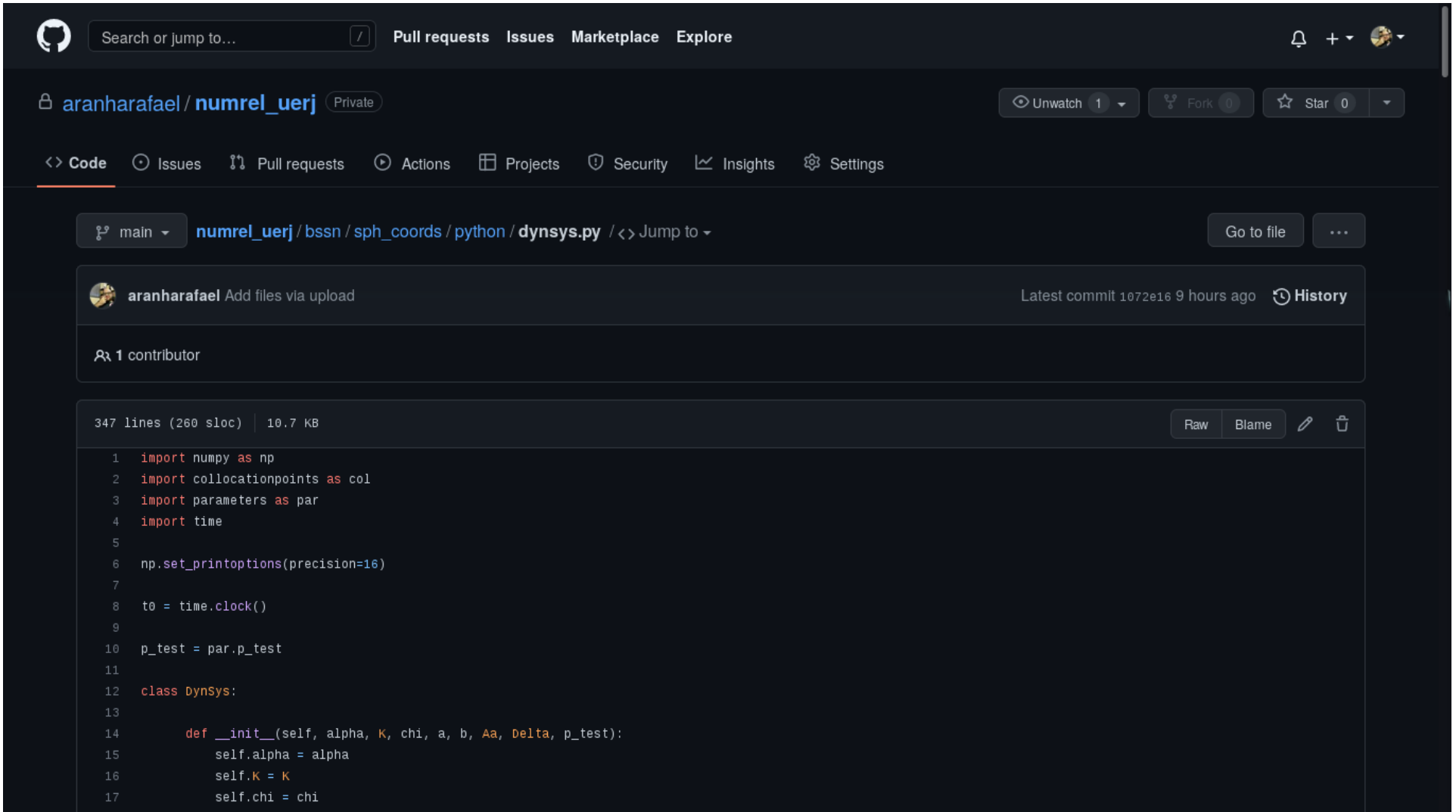

Aplicação

Aplicação - Código Rio

- Código **RIO** para simetria esférica no vácuo: G-BSSN + Spectral Methods

New numerical framework for the generalized Baumgarte-Shapiro-Shibata-Nakamura formulation: The vacuum case for spherical symmetry

M. A. Alcoforado,[1] R. F. Aranha,[1] W. O. Barreto,[1,2] and H. P. de Oliveira[1]

[1]*Departamento de Física Teórica, Universidade do Estado do Rio de Janeiro, Rua São Francisco Xavier 524, 20550-013 Maracanã, Rio de Janeiro, RJ, Brazil*

[2]*Centro de Física Fundamental, Universidad de Los Andes, Mérida 5101, Venezuela*

(Received 19 May 2021; revised 20 August 2021; accepted 28 September 2021; published 18 October 2021)

Here we report a developed high performance and simplified version of the code denominated RIO, which can be easily extended, for the generalized BSSN formulation. We implement a code which is regular at the center of symmetry, without use a special procedure for regularization, as usual. We get exponential convergence for constraints. The numerical algorithm is based on the Galerkin-Collocation method developed successfully for diverse physical scenarios by the Numerical Relativity Group at UERJ. For the sake of clarity in presentation, we consider here the most simple case to display the most salient features of the procedure. Thus, we focus on the definite tests of the new numerical framework. The timing and performance of the code show that we can reach a better accuracy close to the machine precision, for the Hamiltonian and momentum constraints. RIO will be an open source code; currently it is under continuous development to consider more general and realistic problems.

DOI: 10.1103/PhysRevD.104.084065

- Calibração para um dado inicial de **pura gauge** (lapso não nulo e shift nulo.)

Aplicação - equações BSSN

- Métrica esfericamente simétrica:

$$ds^2 = -\alpha^2 dt^2 + \psi^4 (A dr^2 + B r^2 d\Omega), \qquad (1)$$

- Equações BSSN

$$\partial_t \alpha = -\alpha^2 K, \qquad (2)$$

$$\partial_t A = -2\alpha \tilde{A}_{rr}, \qquad (3)$$

$$\partial_t B = -2\alpha \tilde{A}_{\theta\theta}, \qquad (4)$$

$$\partial_t \psi = -\frac{1}{6}\alpha \psi K, \qquad (5)$$

$$\partial_t \tilde{\Lambda} = \frac{2\alpha}{A}\left(\frac{6\tilde{A}_{\theta\theta}}{A}\frac{\partial_r \psi}{\psi} - \frac{2}{3}\partial_r K\right) + \frac{\alpha}{A}\left(\frac{\tilde{A}_{rr}\partial_r A}{A^2} - \frac{2\tilde{A}_{\theta\theta}\partial_r B}{B^2} + \frac{4\tilde{A}_{\theta\theta}(A-B)}{rB^2}\right) - \frac{2\tilde{A}_{rr}\partial_r \alpha}{A^2}, \qquad (6)$$

$$\partial_t \tilde{A}_{rr} = \frac{1}{\psi^4}[-\mathcal{D}^{TF}_{rr} + \alpha R^{TF}_{rr}] + \alpha\left(\tilde{A}_{rr}K - \frac{2\tilde{A}^2_{rr}}{A}\right), \qquad (7)$$

$$\partial_t \tilde{A}_{\theta\theta} = \frac{1}{r^2\psi^4}[-D^{TF}_{\theta\theta} + \alpha R^{TF}_{\theta\theta}] + \alpha\left(\tilde{A}_{\theta\theta}K - \frac{2\tilde{A}^2_{\theta\theta}}{B}\right), \qquad (8)$$

$$\partial_t K = \alpha\left(\frac{1}{3}K^2 + \frac{\tilde{A}^2_{rr}}{A^2} + \frac{2\tilde{A}^2_{\theta\theta}}{B^2}\right) - \mathcal{D}, \qquad (9)$$

- Derivada covariante e Ricci:

$$\mathcal{D} = \frac{1}{\psi^4}\left(\frac{\mathcal{D}_{rr}}{A} + \frac{2\mathcal{D}_{\theta\theta}}{r^2 B}\right), \qquad (10)$$

$$\mathcal{D}_{rr} = \partial_r^2 \alpha - \frac{(\partial_r \alpha)}{2}\left(\frac{\partial_r A}{A} + \frac{4\partial_r \psi}{\psi}\right), \qquad (11)$$

$$\mathcal{D}_{\theta\theta} = \frac{r(\partial_r \alpha)}{A}\left[B + \frac{r}{2}\left(\partial_r B + 4B\frac{\partial_r \psi}{\psi}\right)\right], \qquad (12)$$

$$R_{rr} = \frac{3(\partial_r A)^2}{4A^2} - \frac{(\partial_r B)^2}{2B^2} + A\partial_r \tilde{\Lambda} + \frac{1}{2}\tilde{\Lambda}\partial_r A + \frac{1}{r}\left[-4\left(\frac{\partial_r \psi}{\psi}\right) - \frac{1}{B}(\partial_r A + 2\partial_r B) + \frac{2A\partial_r B}{B^2}\right] - 4\partial_r\left(\frac{\partial_r \psi}{\psi}\right) + 2\left(\frac{\partial_r \psi}{\psi}\right)\left(\frac{\partial_r A}{A} - \frac{\partial_r B}{B}\right) - \frac{\partial_r^2 A}{2A} + \frac{2(A-B)}{r^2 B}, \qquad (13)$$

$$R_{\theta\theta} = \frac{r^2 B}{A}\left[\frac{\partial_r \psi}{\psi}\frac{\partial_r A}{A} - 2\partial_r\left(\frac{\partial_r \psi}{\psi}\right) - 4\left(\frac{\partial_r \psi}{\psi}\right)^2\right] + \frac{r^2}{A}\left[\frac{(\partial_r B)^2}{2B} - 3\frac{\partial_r \psi}{\psi}\partial_r B - \frac{1}{2}\partial_r^2 B + \frac{1}{2}\tilde{\Lambda}A\partial_r B\right] + r\left(\tilde{\Lambda}B - \frac{\partial_r B}{B} - 6\frac{\partial_r \psi}{\psi}\frac{B}{A}\right) + \frac{B}{A} - 1. \qquad (14)$$

Aplicação - vínculos

- Vínculo hamiltoniano:

$$\mathcal{H} \equiv \frac{2}{3}K^2 - \frac{\tilde{A}_{rr}^2}{A^2} - \frac{2\tilde{A}_{\theta\theta}^2}{B^2} + \frac{1}{\psi^4}\left(\partial_r\tilde{\Lambda} + \frac{1}{2}\tilde{\Lambda}\frac{\partial_r A}{A} + \tilde{\Lambda}\frac{\partial_r B}{B} + \frac{2\tilde{\Lambda}}{r}\right) - \frac{8}{A\psi^5}\left(\partial_r^2\psi - \frac{1}{2}\frac{(\partial_r A)\partial_r\psi}{A} + \frac{(\partial_r B)\partial_r\psi}{B} + \frac{2\partial_r\psi}{r}\right) - \frac{1}{A\psi^4}\left(\frac{1}{2}\frac{\partial_r^2 A}{A} - \frac{3}{4}\frac{(\partial_r A)^2}{A^2} + \frac{\partial_r^2 B}{B} - \frac{1}{2}\frac{(\partial_r B)^2}{B^2} + \frac{2\partial_r B}{rB} + \frac{\partial_r A}{rB}\right) = 0, \quad (17)$$

- Vínculo de momento:

$$\mathcal{M}^r \equiv \frac{2}{3}\partial_r K - \frac{\partial_r\tilde{A}_{rr}}{A} - 6\frac{\tilde{A}_{rr}}{A}\frac{\partial_r\psi}{\psi} + \frac{\tilde{A}_{rr}\partial_r A}{A^2} - \frac{(\partial_r B)\tilde{A}_{rr}}{AB} + \frac{(\partial_r B)\tilde{A}_{\theta\theta}}{B^2} - \frac{2\tilde{A}_{rr}}{rA} + \frac{2\tilde{A}_{\theta\theta}}{rB} = 0. \quad (18)$$

- Vínculos "acidentais":

$$\tilde{A}_{rr}/A + 2\tilde{A}_{\theta\theta}/B = 0 \ (\tilde{A}_{ij} \text{ is trace-free}) \quad (19)$$

$$\tilde{\Lambda} = \frac{1}{A}\left[\frac{\partial_r A}{2A} - \frac{\partial_r B}{B} - \frac{2}{r}\left(1 - \frac{A}{B}\right)\right], \quad (20)$$

Aplicação - condições de contorno

- Conformalmente plana na origem e determinante da métrica 3D constante:

$$A(t,0) = B(t,0) = 1$$

- Na origem (r=0):

$$\tilde{A}_{rr}(t,0) = \tilde{A}_{\theta\theta}(t,0) = 0,$$

$$\partial_r A(t,r)|_{r=0} = \partial_r B(t,r)|_{r=0} = 0,$$

$$\partial_r \tilde{A}_{rr}(t,r)|_{r=0} = \partial_r \tilde{A}_{\theta\theta}(t,r)|_{r=0} = 0,$$

$$\tilde{\Lambda}(t,0) = 0,$$

$$\partial_r K(t,r)|_{r=0} = \partial_r \psi(t,r)|_{r=0} = 0.$$

- No infinito (r→ inf):

$$A = B = \psi = \alpha = 1, \quad \text{at: } (t,\infty)$$

$$\tilde{A}_{rr} = \tilde{A}_{\theta\theta} = K = \tilde{\Lambda} = 0, \quad \text{at: } (t,\infty).$$

Aplicações - Paridade das variáveis BSSN

- Análise das condições de contorno nas equações BSSN:

$$\alpha(t,r) = \alpha_0(t) + \alpha_2(t) r^2 + \mathcal{O}(r^4)$$

- Paridade par:

$$K(t,r) = K_0(t) + K_2(t) r^2 + \mathcal{O}(r^4),$$

$$\chi(t,r) = \chi_0(t) + \chi_2(t) r^2 + \mathcal{O}(r^4),$$

$$A(t,r) = 1 + \mathcal{O}(r^2),$$

$$B(t,r) = 1 + \mathcal{O}(r^2),$$

$$A_a(t,r) = \mathcal{O}(r^2).$$

- Paridade ímpar:

$$\hat{\Delta}(t,r) = \hat{\Delta}_1(t) r + \mathcal{O}(r^3).$$

Aplicação - Expansão na base apropriada

- "Super Base":

$$SB_0(r) = \left(1 + \frac{r^2}{L_0^2}\right)^{-\frac{1}{2}} \qquad SB_1(r) = \frac{2r}{L_0}\left(1 + \frac{r^2}{L_0^2}\right)^{-1}$$

$$SB_{n+1}(r) = \frac{2r}{L_0}\left(1 + \frac{r^2}{L_0^2}\right)^{-\frac{1}{2}} SB_n(r) - SB_{n-1}(r)$$

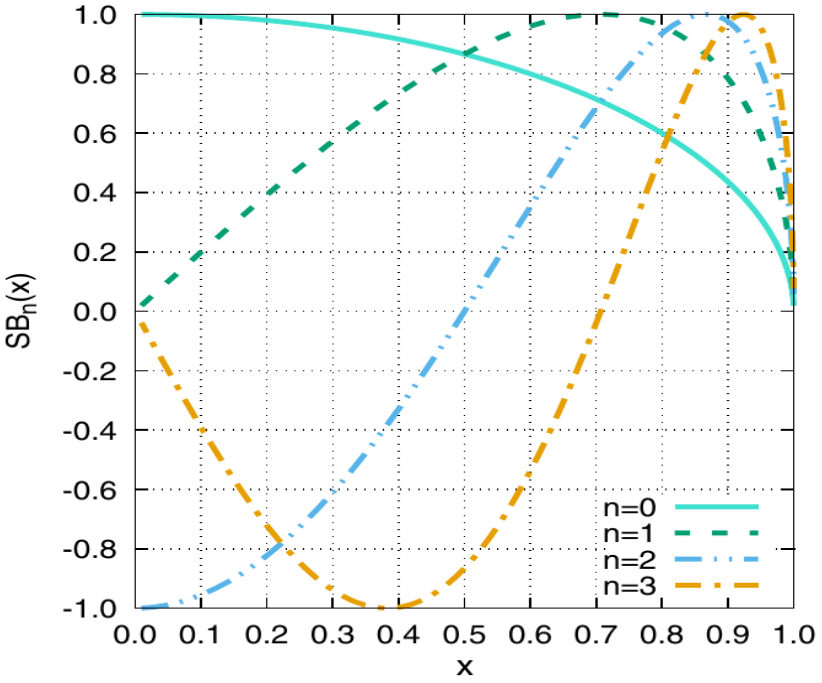

- Expansão das variáveis BSSN:

$$\alpha_N(t,r) = 1 + \sum_{j=0}^{N} \hat{\alpha}_j(t) SB_{2j}(r), \qquad (42)$$

$$\chi_N(t,r) = \sum_{j=0}^{N} \hat{\chi}_j(t) SB_{2j}(r), \qquad (43)$$

$$K_N(t,r) = \sum_{j=0}^{N} \hat{K}_j(t) SB_{2j}(r), \qquad (44)$$

$$A_N(t,r) = 1 + \frac{1}{2}\sum_{j=0}^{N-1} \hat{A}_j(t)(SB_{2j+2}(r) - SB_{2j}(r)), \qquad (45)$$

$$B_N(t,r) = 1 + \frac{1}{2}\sum_{j=0}^{N-1} \hat{B}_j(t)(SB_{2j+2}(r) - SB_{2j}(r)), \qquad (46)$$

$$A_{aN}(t,r) = \frac{1}{2}\sum_{j=0}^{N-1} \hat{A}_{aj}(t)(SB_{2j+2}(r) - SB_{2j}(r)), \qquad (47)$$

$$\Delta_N(t,r) = \sum_{j=0}^{N-1} \hat{\Delta}_j(t) SB_{2j+1}(r). \qquad (48)$$

Aplicação - Pontos de colocação

- Pontos de colocação

$$r_k = \frac{L_0 x_k}{\sqrt{1 - x_k^2}} \qquad x_k = \cos\left(\frac{\pi k}{2N+2}\right), \quad k = 0, 1, \ldots, 2N+2$$

- Substituição dos pontos de colocação nas equações BSSN:

$$\alpha_k(t) = 1 + \sum_{j=0}^{N} \hat{\alpha}_j(t) SB_{2j}(r_k) \quad \bullet \rightarrow$$

$$\begin{pmatrix} \alpha_1 \\ \alpha_2 \\ \vdots \\ \alpha_{N+1} \end{pmatrix} = \begin{pmatrix} 1 \\ 1 \\ \vdots \\ 1 \end{pmatrix} + \mathbb{AL} \begin{pmatrix} \hat{\alpha}_1 \\ \hat{\alpha}_2 \\ \vdots \\ \hat{\alpha}_{N+1} \end{pmatrix}$$

$$\mathbb{AL}_{kj} = SB_{2j}(r_k)$$

- Pontos de colocação:

$$(\partial_t \alpha)_k = -\alpha_k^2 K_k, \quad k = 1, 2, \ldots, N+1$$

Esquema de integração:

- (I) Condições iniciais para os coeficientes espectrais;
- (II) Derivadas temporais iniciais dos coeficientes espectrais;
- (III) Obtenção dos novos coeficientes modais via Runge-Kutta (Cash-Karp);

Aplicação - Convergência dos dados iniciais

- Dado inicial (pura gauge):

$$\alpha(0,r) = 1 + \frac{\alpha_i r^2}{1+r^2}\left[e^{-(r-r_0)^2/\sigma^2} + e^{-(r-r_0)^2/\sigma^2}\right]$$

- Convergência:

$$\|\ldots\|_2 = \left\{\frac{1}{2}\int_0^\infty (\ldots)^2 dr\right\}^{1/2}$$

- Erro L2

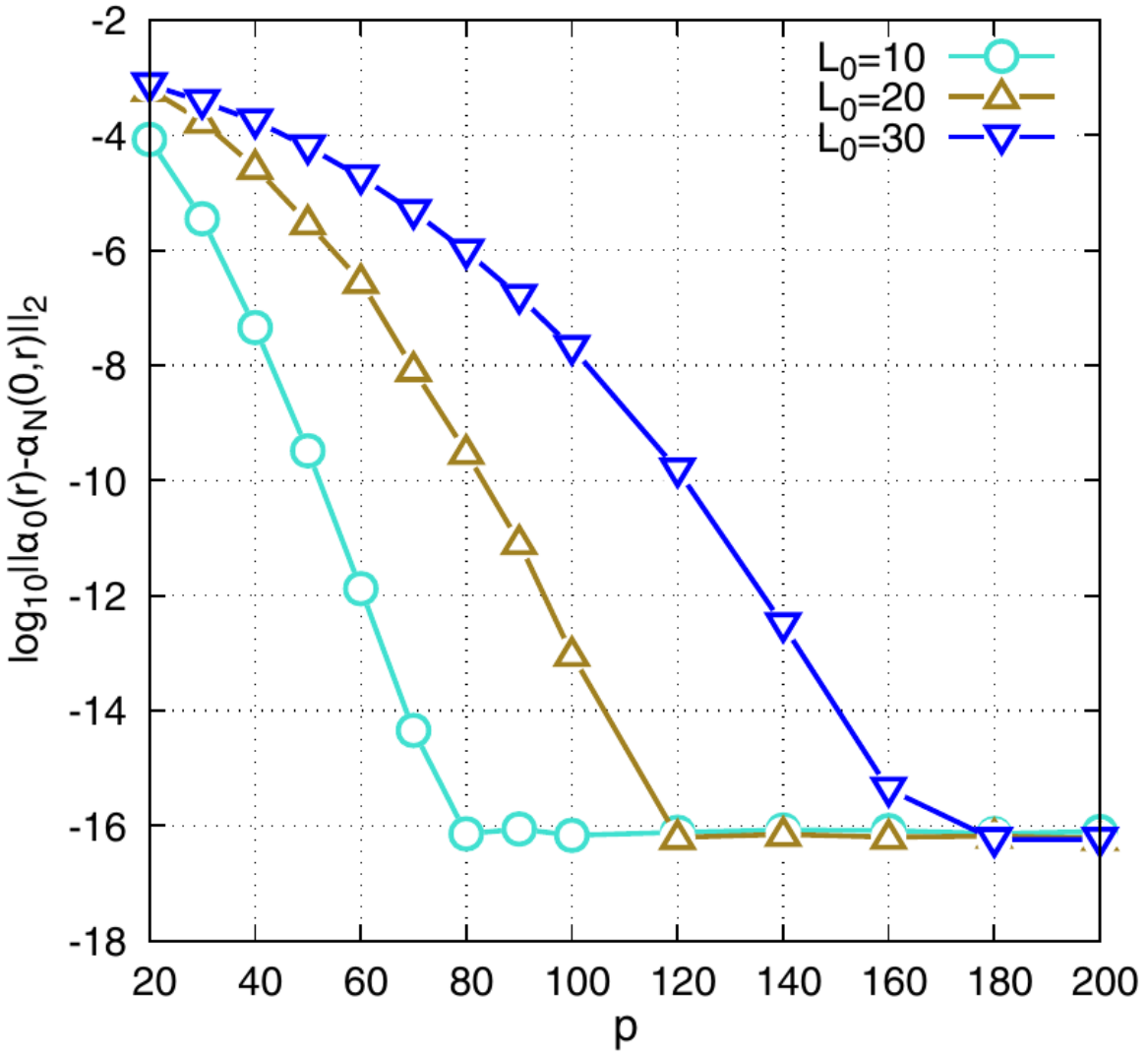

Aplicação - Evolução do lapso

- Separação em dois pulsos:

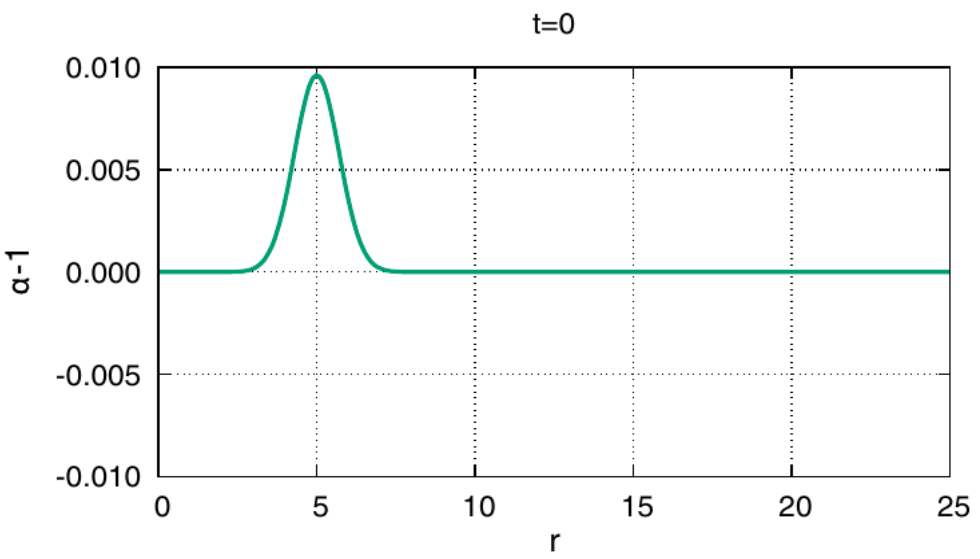

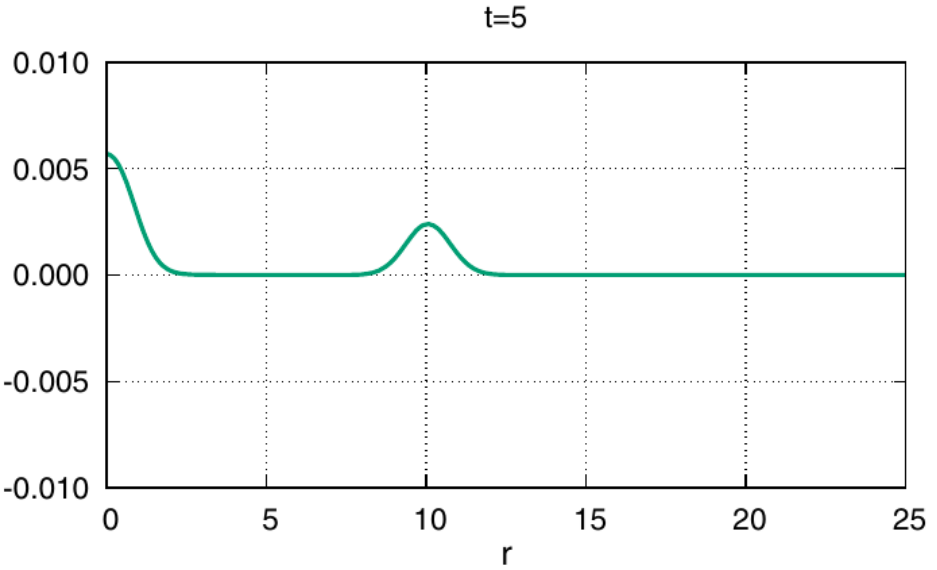

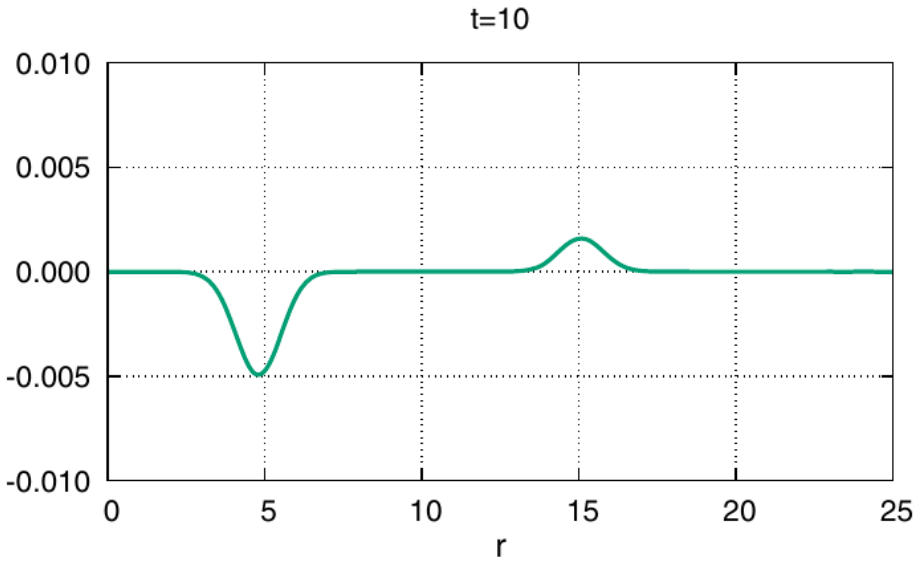

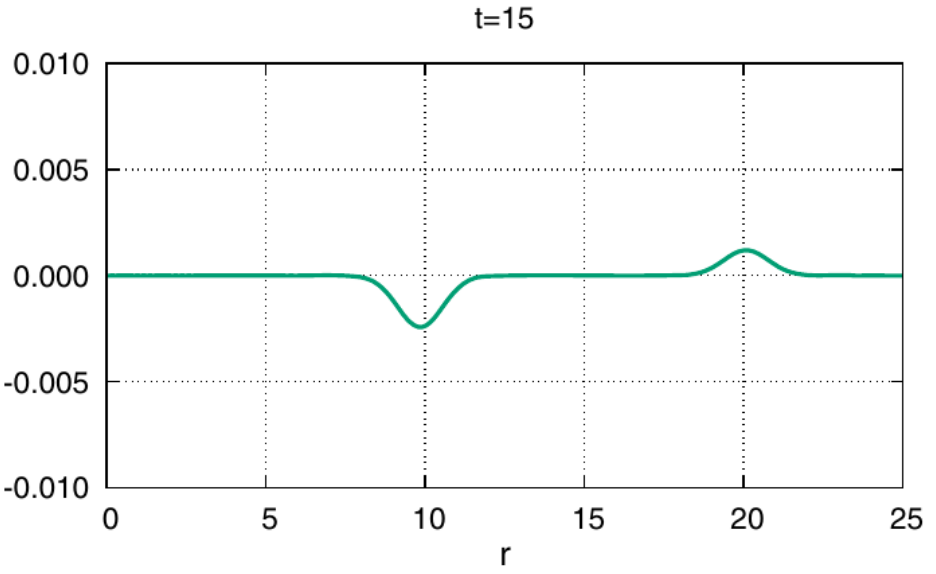

Aplicação - Vínculo hamiltoniano e de momento

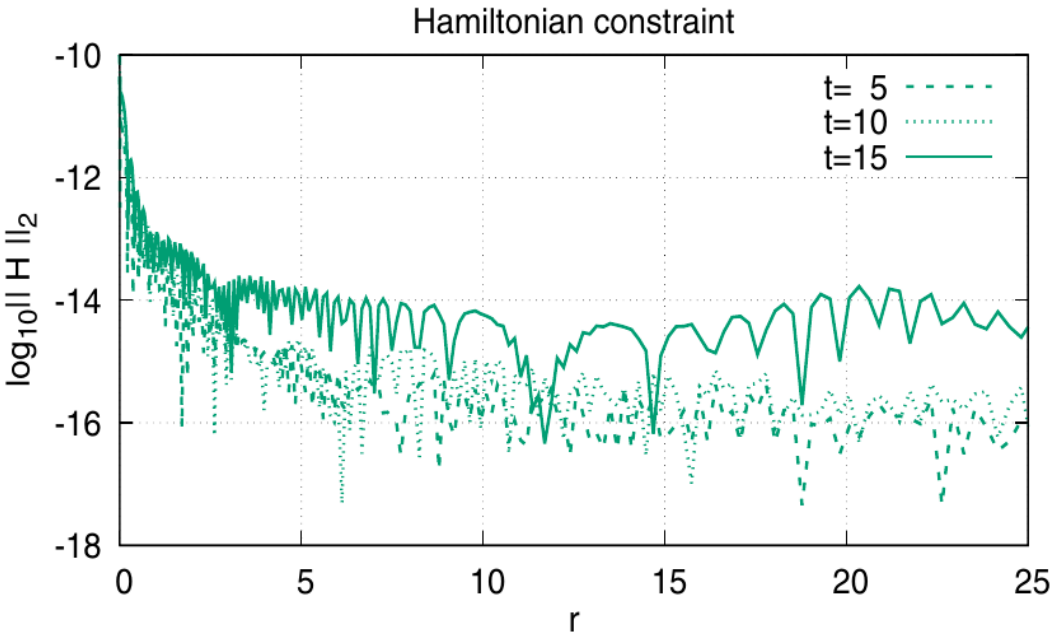

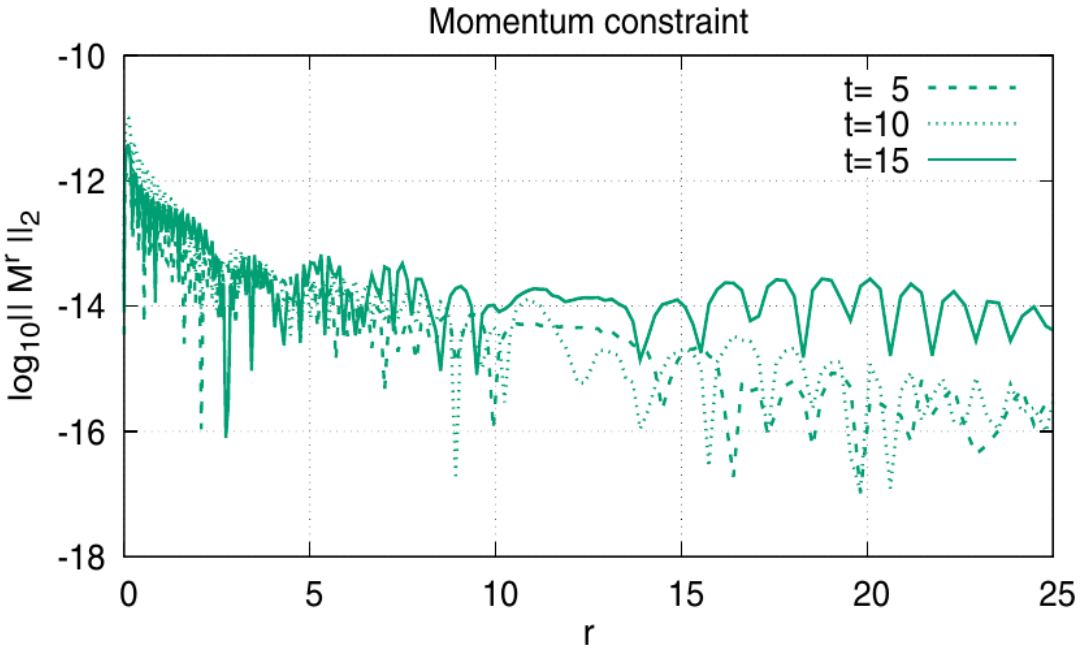

Aplicação - Convergência dos vínculos

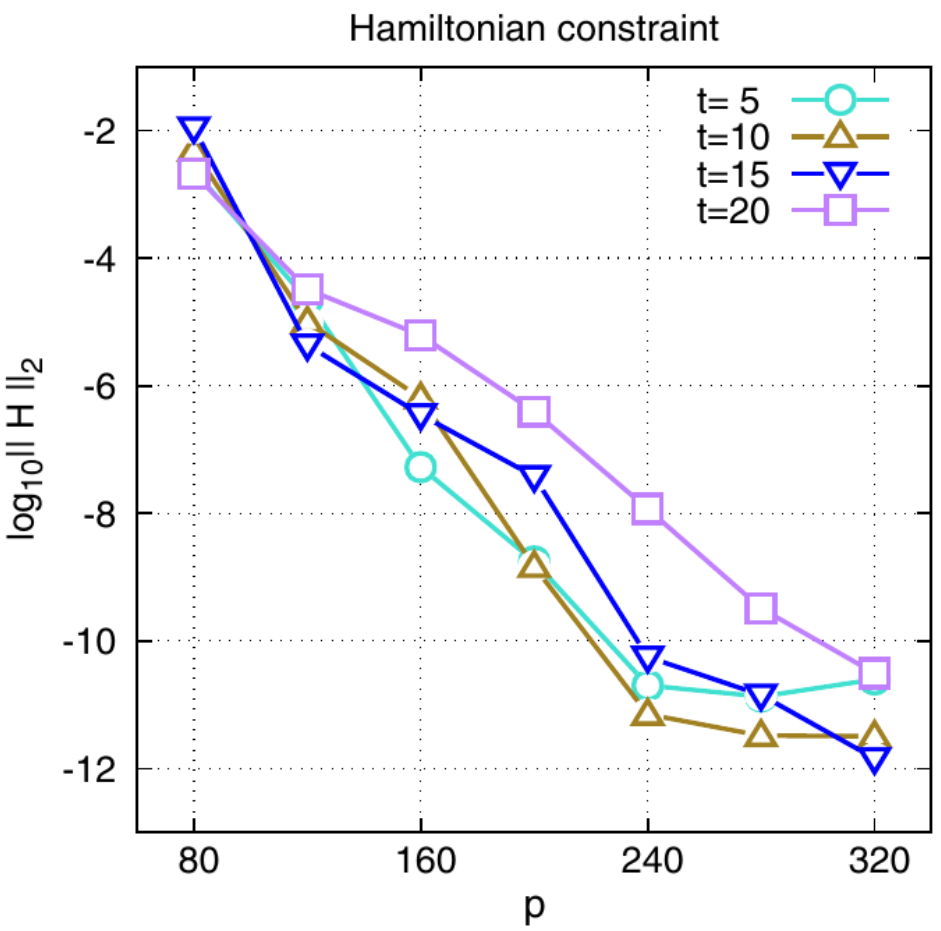

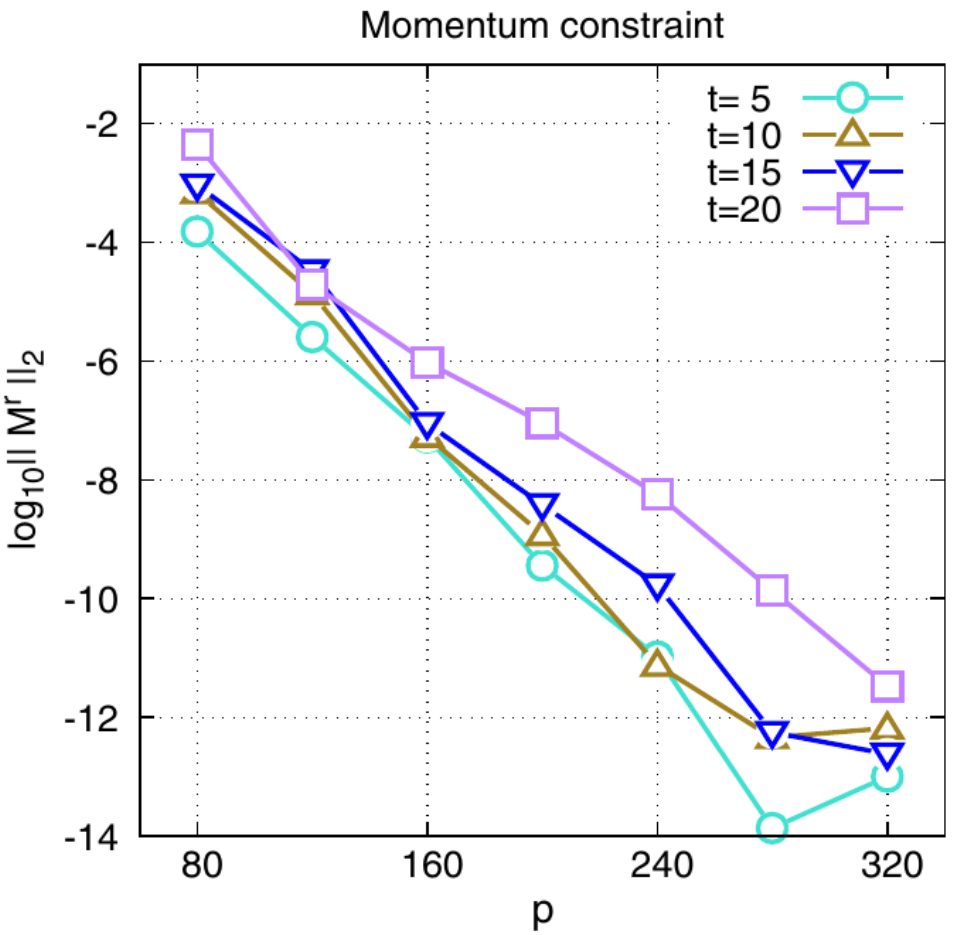

- Em cada tempo de integração numérica os vínculos convergem exponencialmente!

5
Considerações Finais

Próximos passos

Metas específicas (curto prazo):

- Verificação do fenômeno crítico no colapso.
- Comportamento do campo escalar para diferentes potenciais.
- Explorar caso de simetria axial (code cyl_coords).
- Ondas de Brill e Teukolsky.

Metas gerais:

- Explorar outros "benchmarks": BBN, RNS, GW, BBH.
- Divulgação: webpage, repositório no GitHub.
- Criação de cursos de NumRel (todos os níveis).
- Implementação de GPU's.
- Manutenção periódica dos códigos.
- Ampliação de colaborações.

Bibliografia

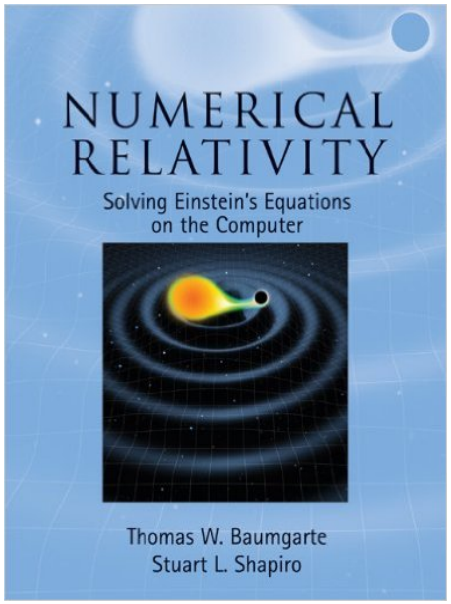

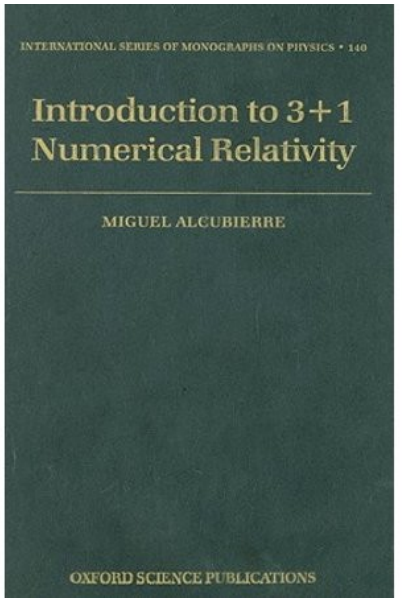

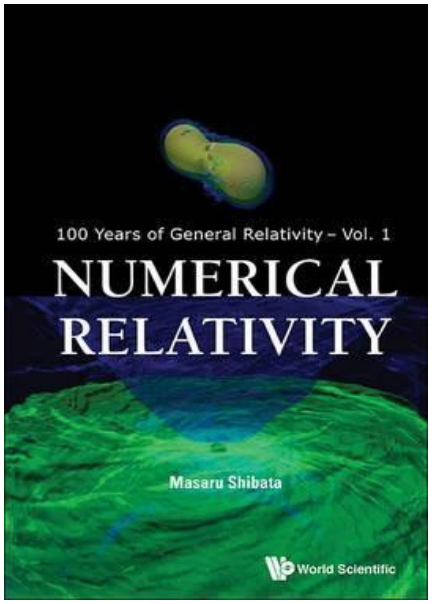

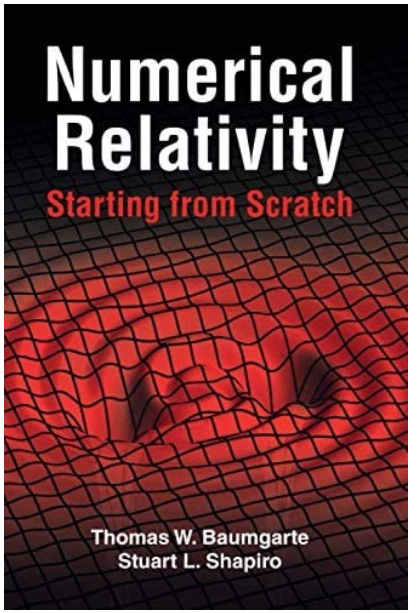

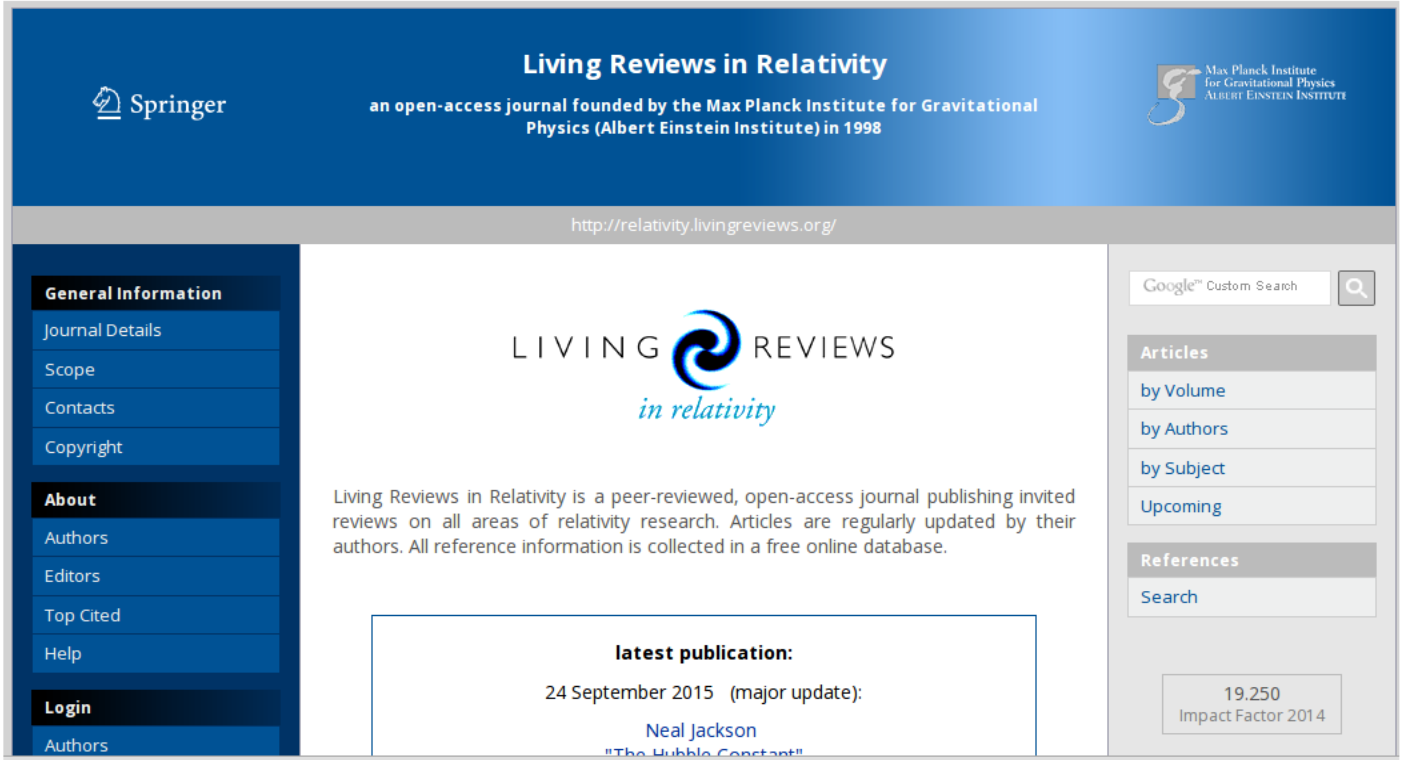

Bondi-Sachs Formulation (Characteristic, 2+1+1):

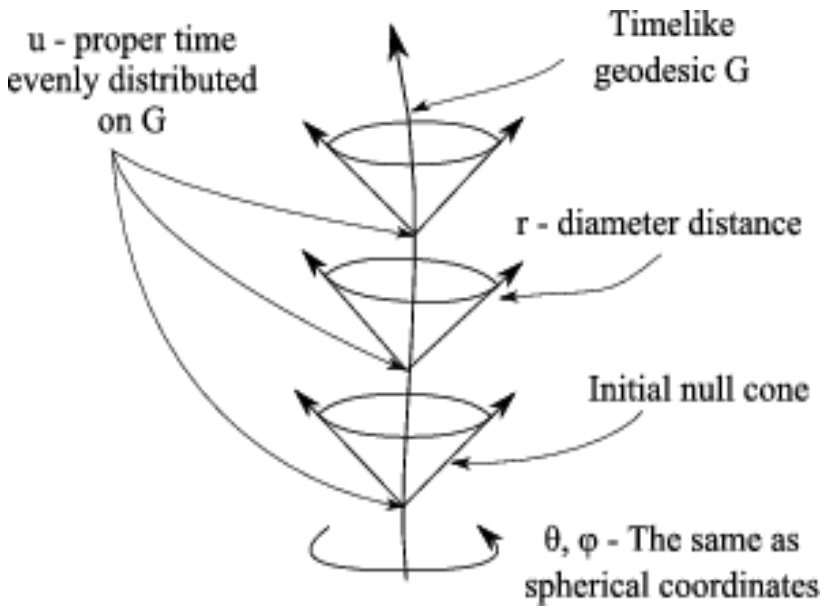

Bondi metric:

$$ds^2 = (\frac{V}{r}e^{2\beta} - U^2 r^2 e^{2\gamma})du^2 + 2e^{2\beta}dudr + 2Ur^2 e^{2\gamma}dud\theta - r^2(e^{2\gamma}d\theta^2 + e^{-2\gamma}\sin^2\theta d\phi^2)$$

Surface equations:

$$\beta_{,r} = \frac{1}{2}r\,(\gamma_{,r})^2$$

$$[r^4 e^{2(\gamma-\beta)}U_{,r}]_{,r} = 2r^2[r^2(\frac{\beta}{r^2})_{,r\theta} - \frac{(\sin^2\theta\,\gamma)_{,r\theta}}{\sin^2\theta} + 2\,\gamma_{,r}\,\gamma_{,\theta})]$$

$$V_{,r} = -\frac{1}{4}r^4 e^{2(\gamma-\beta)}(U_{,r})^2 + \frac{(r^4\sin\theta U)_{,r\theta}}{2r^2\sin\theta} + e^{2(\beta-\gamma)}[1 - \frac{(\sin\theta\beta_{,\theta})_{,\theta}}{\sin\theta} + \gamma_{,\theta\theta} + 3\cot\theta\gamma_{,\theta} - (\beta_{,\theta})^2 - 2\gamma_{,\theta}(\gamma_{,\theta} - \beta_{,\theta})]$$

Dynamical equation:

$$4r(r\gamma)_{,ur} = [2r\gamma_{,r}V - r^2(2\gamma_{,\theta}U + \sin\theta(\frac{U}{\sin\theta})_{,\theta})]_{,r} - 2r^2\frac{(\gamma_{,r}U\sin\theta)_{,\theta}}{\sin\theta} + \frac{1}{2}r^4 e^{2(\gamma-\beta)}(U_{,r})^2 + 2e^{2(\beta-\gamma)}[(\beta_{,\theta})^2 + \sin\theta(\frac{\beta_{,\theta}}{\sin\theta})_{,\theta}]$$

Advs: Evolution along null geodesics, absence of constraint equations.
Disadvs: Development of caustics, less intuitive, initial data.